

Spring 5-31-2018

## Mechanochemical nitration of aromatic compounds

Oleg Shlomo Lagoviyer  
*New Jersey Institute of Technology*

Follow this and additional works at: <https://digitalcommons.njit.edu/theses>

 Part of the [Chemical Engineering Commons](#)

---

### Recommended Citation

Lagoviyer, Oleg Shlomo, "Mechanochemical nitration of aromatic compounds" (2018). *Theses*. 1574.  
<https://digitalcommons.njit.edu/theses/1574>

This Thesis is brought to you for free and open access by the Electronic Theses and Dissertations at Digital Commons @ NJIT. It has been accepted for inclusion in Theses by an authorized administrator of Digital Commons @ NJIT. For more information, please contact [digitalcommons@njit.edu](mailto:digitalcommons@njit.edu).

## **Copyright Warning & Restrictions**

The copyright law of the United States (Title 17, United States Code) governs the making of photocopies or other reproductions of copyrighted material.

Under certain conditions specified in the law, libraries and archives are authorized to furnish a photocopy or other reproduction. One of these specified conditions is that the photocopy or reproduction is not to be “used for any purpose other than private study, scholarship, or research.” If a user makes a request for, or later uses, a photocopy or reproduction for purposes in excess of “fair use” that user may be liable for copyright infringement,

This institution reserves the right to refuse to accept a copying order if, in its judgment, fulfillment of the order would involve violation of copyright law.

**Please Note: The author retains the copyright while the New Jersey Institute of Technology reserves the right to distribute this thesis or dissertation**

Printing note: If you do not wish to print this page, then select “Pages from: first page # to: last page #” on the print dialog screen

The Van Houten library has removed some of the personal information and all signatures from the approval page and biographical sketches of theses and dissertations in order to protect the identity of NJIT graduates and faculty.

## **ABSTRACT**

### **MECHANOCHEMICAL NITRATION OF AROMATIC COMPOUNDS**

**by**  
**Oleg Shlomo Lagoviyer**

Aromatic compounds such as toluene are commercially nitrated using a combination of nitric acid with other strong acids. This process relies on the use of highly corrosive chemicals and generates environmentally harmful waste, which is difficult to handle and dispose of. In this study aromatic nitration using solvent-free mechanochemical processing of environmentally benign precursors has been achieved and investigated. Mononitrotoluene was synthesized by milling toluene with sodium nitrate and molybdenum trioxide as a catalyst. Several parameters affecting the desired product yield and selectivity were identified and varied. MNT yields in excess of 60% have been achieved in different tests. The desired product yield and selectivity were found to strongly depend on the ratios of the reactants and the catalyst. A parametric study addressed the effects of milling time, temperature, milling media, and catalyst additives on the MNT yield and on the formation of various byproducts. Toluene conversion as a function of milling time exhibited a maximum, which occurred earlier for smaller milling balls. Milling temperature had only a weak effect on MNT formation, but affected the formation of other aromatic byproducts. Replacing various fractions of  $\text{MoO}_3$  with fumed silica led to an increased yield of MNT for up to 30% of silica. The yield dropped when higher percentages of  $\text{MoO}_3$  were replaced. The degree of refinement of  $\text{MoO}_3$  attained in the mill has been quantified by measuring the surface area of the inorganic fraction of the milled material. The surface measurements were correlated with the product yield.

# **MECHANOCHEMICAL NITRATION OF AROMATIC COMPOUNDS**

by  
**Oleg Shlomo Lagoviyer**

**A Thesis  
Submitted to the Faculty of New Jersey Institute of Technology  
in Partial Fulfilment of the Requirements for  
Master of Science Degree in Chemical Engineering**

**Otto H. York Department of Chemical, Biological, and Pharmaceutical Engineering**

**May 2018**

Blank Page

## **APPROVAL PAGE**

### **MECHANOCHEMICAL NITRATION OF AROMATIC COMPOUNDS**

**Oleg Shlomo Lagoviyer**

---

|   |      |
|---|------|
| Dr. Edward L. Dreizin, Thesis Advisor<br>Distinguished Professor, Associate Chair of Graduate Studies, Otto H. York Department<br>of Chemical, Biological, and Pharmaceutical Engineering, NJIT | Date |
|---|------|

---

|  |      |
|--|------|
| Dr. Lisa B. Axe,<br>Chair Person and Professor, Otto H. York Department of Chemical, Biological, and<br>Pharmaceutical Engineering, NJIT | Date |
|--|------|

---

|   |      |
|---|------|
| Dr. Mirko Schoenitz,<br>Assistant Professor, Otto H. York Department of Chemical, Biological, and<br>Pharmaceutical Engineering, NJIT | Date |
|---|------|

## **BIOGRAPHICAL SKETCH**

**Author:** Oleg Shlomo Lagoviyer

**Degree:** Master of Science

**Date:** May 2018

### **Undergraduate and Graduate Education:**

- Master of Science in Chemical Engineering,  
New Jersey Institute of Technology, Newark, NJ 2018
- Bachelor of Science in Chemical Engineering,  
Missouri University of Science and Technology, Rolla, MO 1995

**Major:** Chemical Engineering

### **Presentations and Publications:**

Lagoviyer, O. S., Krishtopa, L., Schoenitz, M., Trivedi, N. J., Dreizin, E. L.,  
“Mechanochemical Nitration of Aromatic Compounds”, Journal of Energetic  
Materials, July 2017.

Lagoviyer, O. S., Schoenitz, M., Dreizin, E. L., “Effect of milling temperature on structure  
and reactivity of Al–Ni composites”, Journal of Materials Science, 1 January 2018,  
53(2):1178-1190.

Lagoviyer, O. S., Krishtopa, L., Schoenitz, M., Trivedi, N. J., Dreizin, E. L.,  
“Mechanochemical Nitration of Aromatic Compounds”, 2016 Spring Technical  
Meeting of the Eastern States Section of the Combustion Institute, ESSCI 2016.



*To my father, who has always imbued me with love of science.*

## ACKNOWLEDGMENT

First and foremost, I would like to acknowledge the input of my advisor, Dr. Edward L. Dreizin, Distinguished Professor and Associate Chair of Graduate Studies at NJIT. This work would have been impossible without Dr. Dreizin's unwavering dedication, patience, and vast expertise in research and education. The assistance of Dr. Mirko Schoenitz, especially in the experimental aspects of this research, was also invaluable. I would also like to thank Dr. Lisa B. Axe, the Chairperson of Otto H. York Department of Chemical, Biological, and Pharmaceutical Engineering, for her kind encouragement, and valuable advice, especially in editing this publication. Dr. Nirupam J. Trivedi Division Chief at Army Research Laboratory is acknowledged for the original idea behind this study, and for his valuable guidance throughout this effort. Dr. Larissa Krishtopa and Dr. Jeong Seop Shim are acknowledged for allowing the use of the materials characterization laboratory and training me to use the GC-MS and the Nitrogen Adsorption BET instruments. I would also like to thank my father, Dr. Yury Lagoviyer for his warm encouragement, valuable ideas, and assistance in the material analysis.

Finally, I would like to thank the members of my research group: Kerri-Lee Chintersingh-Dinall, Daniel Hastings, Ian Monk, Siva Kumar Valluri, and Song Wang, as well as my family for their constant support and encouragement.

This work was supported by Strategic Environmental Research and Development Program (SERDP) contract W912HQ-17-P-0009. The interest and support of Dr. Robin Nissan, SERDP Program Manager is gratefully acknowledged.

## TABLE OF CONTENTS

| Chapter  | Page |
|--|------|
| 1 LITERATURE REVIEW.....   | 1    |
| 1.1 Introduction: Nitration Reactions.....                                   | 1    |
| 1.2 Shortcomings of Common Nitration Methods.....                            | 2    |
| 1.3 Improved Nitration Methods.....  | 3    |
| 1.4 Mechanochemically Induced Nitration Reactions.....                       | 10   |
| 1.4.1 Mechanochemical Reactions.....   | 10   |
| 1.4.2 Mechanochemical Nitration of Organic Compounds.....                    | 15   |
| 2 MECHANOCHEMICAL NITRATION OF TOLUENE: FEASIBILITY.....                     | 19   |
| 2.1 Introduction.....  | 19   |
| 2.2 Experimental.....  | 22   |
| 2.3 Results.....   | 26   |
| 2.3.1 Formation of Mononitrotoluene with MoO <sub>3</sub> as a Catalyst..... | 26   |
| 2.3.2 Parameters Affecting the Product Yield.....                            | 28   |
| 2.4 Discussion.....  | 34   |
| 2.5 Conclusion.....  | 35   |
| 3 EFFECT OF PROCESS PARAMETERS ON MECHANOCHEMICAL NITRATION OF TOLUENE.....  | 37   |
| 3.1 Introduction.....  | 37   |
| 3.2 Experimental.....  | 39   |
| 3.2.1 Sample Preparation.....  | 39   |
| 3.2.2 Sample Recovery.....   | 41   |

## TABLE OF CONTENTS

(Continued)

| Chapter   | Page |
|---|------|
| 3.2.3 Sample Analysis.....                          | 42   |
| 3.2.4 Surface Area Measurements.....                | 45   |
| 3.3 Results.....                                    | 45   |
| 3.3.1 Preliminary Experiments.....                  | 45   |
| 3.3.2 Effect of Milling Time and Media.....         | 47   |
| 3.3.3 Effect of Temperature.....                    | 49   |
| 3.3.4 Milling with MoO <sub>3</sub> and Silica..... | 51   |
| 3.3.5 Surface Area Measurements.....                | 54   |
| 3.4 Discussion.....                                 | 55   |
| 3.5 Conclusions.....                                | 60   |
| 4 NITRATION OF OTHER AROMATIC COMPOUNDS.....        | 62   |
| 4.1 Naphthalene Nitration.....                      | 62   |
| 4.1.1 Experimental.....                             | 62   |
| 4.1.2 Results and Discussion.....                   | 63   |
| 4.2 Other Compounds.....                            | 66   |
| 4.2.1 Experimental.....                             | 66   |
| 4.2.2 Results.....                                  | 66   |
| 4.2.3 Secondary Nitration.....                      | 68   |

## TABLE OF CONTENTS

(Continued)

|   |    |
|---|----|
| 5 CONCLUSIONS.....                                    | 69 |
| APPENDIX. DERIVATION OF THE MILLING DOSE FORMULA..... | 70 |
| REFERENCES.....                                       | 72 |

## LIST OF TABLES

| Table  | Page |
|--|------|
| 1.1 Conditions and Result of the Liquid Phase Nitration of Toluene.....  | 7    |
| 1.2 Reaction Conditions for Toluene Nitration over $\text{Cs}_{2.5}\text{H}_{0.5}\text{PMoO}_{40}$ Experiments.....              | 8    |
| 1.3 Conditions and Results of Toluene Nitration Using $\text{H}_3\text{PO}_4$ Modified $\text{MoO}_3/\text{SiO}_2$ Catalyst..... | 9    |
| 1.4 Examples of Reactions that Have Been Carried out Mechanochemically.....  | 11   |
| 1.5 List of Aromatic Compounds Nitrated by Albadi, et al.....  | 16   |
| 2.1 Summary of the Milling Conditions for 2 hr Runs.....   | 24   |
| 2.2 Specific Surface Area of Unmilled and Milled $\text{MoO}_3$ Samples.....   | 34   |
| 3.1 Milling Media.....   | 39   |
| 3.2 Temperature Control Regimes of Planetary Mill Experiments.....   | 41   |
| 3.3 Summary of Systematic Experiment Data.....   | 46   |
| 3.4 Selected Surface Area Measurements and Surface Coverage Estimates.....   | 60   |
| 4.1 Milling Equipment and Operating Conditions.....  | 63   |

## LIST OF FIGURES

| Figure  | Page |
|---|------|
| 1.1 Vapor phase nitration of toluene.....   | 4    |
| 1.2 Vapor phase nitration of toluene with zeolite catalysts.....                                      | 5    |
| 1.3 Nitration over preshaped silica impregnated with H <sub>2</sub> SO <sub>4</sub> .....             | 6    |
| 1.4 Vapor phase nitration over mordenite.....   | 6    |
| 1.5 Effect of reaction time on the conversion of toluene over CsPMA-10/SiO <sub>2</sub> ....          | 8    |
| 1.6 Knoevenagel condensation.....   | 12   |
| 1.7 Direct oxidative amidation.....   | 12   |
| 1.8 Solvent-free peptide synthesis.....   | 13   |
| 1.9 Fullerene dimerization.....   | 13   |
| 1.10 Solvent-free ball milling synthesis of a large organic cage.....                                 | 14   |
| 2.1 Ternary diagram showing relative amounts of the reactants in the 2 hr<br>milling experiments..... | 26   |
| 2.2 GC-MS traces for selected mechanochemical experiments on nitration of<br>toluene.....             | 27   |
| 2.3 Mononitrotoluene yield and selectivity vs NaNO <sub>3</sub> /toluene molar ratio.....             | 30   |
| 2.4 MNT yield and selectivity vs. MoO <sub>3</sub> /NaNO <sub>3</sub> molar ratio.....                | 30   |
| 2.5 MNT yield and selectivity vs. MoO <sub>3</sub> /toluene molar ratio.....                          | 31   |
| 2.6 Selectivity vs. MNT yield.....  | 32   |
| 2.7 MNT yield and selectivity vs. milling dose.....   | 33   |
| 3.1 Sample GC-MS trace of a processed sample with xylene added as an internal<br>standard.....        | 43   |

## LIST OF FIGURES

(Continued)

| Figure   | Page |
|--|------|
| 3.2 Absolute MNT yield for different milling times and milling media.....  | 48   |
| 3.3 Total byproduct recovery, MNT yield, depletion of toluene, and yield of significant byproducts as functions of milling time.....                                 | 49   |
| 3.4 Total product recovery, MNT yield, depletion of toluene along with yield of significant byproducts as functions of milling temperature.....                      | 50   |
| 3.5 MNT yield vs. fraction of Silica.....  | 52   |
| 3.6 Product recovery, MNT yield, depletion of toluene, and significant byproduct yields as functions of added silica.....  | 53   |
| 3.7 Product recovery, MNT yield, toluene consumption, and byproduct yields as functions of milling temperature.....  | 54   |
| 3.8 MNT yield as a function of surface area of the milled solids.....  | 55   |
| 4.1 Sample GC traces for the products of cryogenic naphthalene nitration using $\text{AlCl}_3$ and room temperature shaker mill nitration using $\text{MoO}_3$ ..... | 64   |
| 4.2 Nitronaphthalene yield as a function of milling dose for the experiments carried out in the shaker mill.....   | 65   |
| 4.3 GC trace for the anisole nitration sample. Catalyst: pure $\text{MoO}_3$ .....   | 67   |
| 4.4 GC trace for the anisole nitration sample. Catalyst: 70% $\text{MoO}_3$ 30% $\text{SiO}_2$ .....   | 67   |



# **CHAPTER 1**

## **LITERATURE REVIEW**

### **1.1 Introduction: Nitration Reactions**

Some of the most common and important organic reactions involve nitration of various organic compounds [1]. Nitrated organic compounds find wide use in many applications. Majority of energetic materials, for example, are organic compounds, which derive their energy from the nitro group serving as an intramolecular oxidizer [2]. Nitrated aromatics are of particular interest as they are widely used as solvents, dyes [3], explosives [4], pharmaceuticals [5], and perfumes [6]. In addition, they serve as intermediates in preparation of other compounds, particularly amines [6]. Nitrotoluene (NT), for example, is the first precursor in the synthesis of trinitrotoluene – a common explosive [7, 8]. In addition, NT is used in synthesis of toluidine, nitrobenzaldehyde, and chloronitrotoluenes, which are the intermediates for the production of dyes, resin modifiers, optical brighteners and suntan lotions [9]. Other nitrated compounds, such as nitrocellulose and nitroglycerine also have a number of applications in energetic formulations (propellants, explosives, pyrotechnics) [10] and in pharmaceuticals [11]. The nitrating agent for these reactions has traditionally been fuming nitric acid combined with another strong acid, e.g., sulfuric acid, perchloric acid, selenic acid, hydrofluoric acid, boron trifluoride, or an ion-exchange resin containing sulfonic acid groups. These strong acids are catalysts that result in formation of nitronium ion,  $\text{NO}_2^+$ . Sulfuric acid is almost always used industrially since it is both effective and relatively inexpensive [12, 13].

## 1.2 Shortcomings of Common Nitration Methods

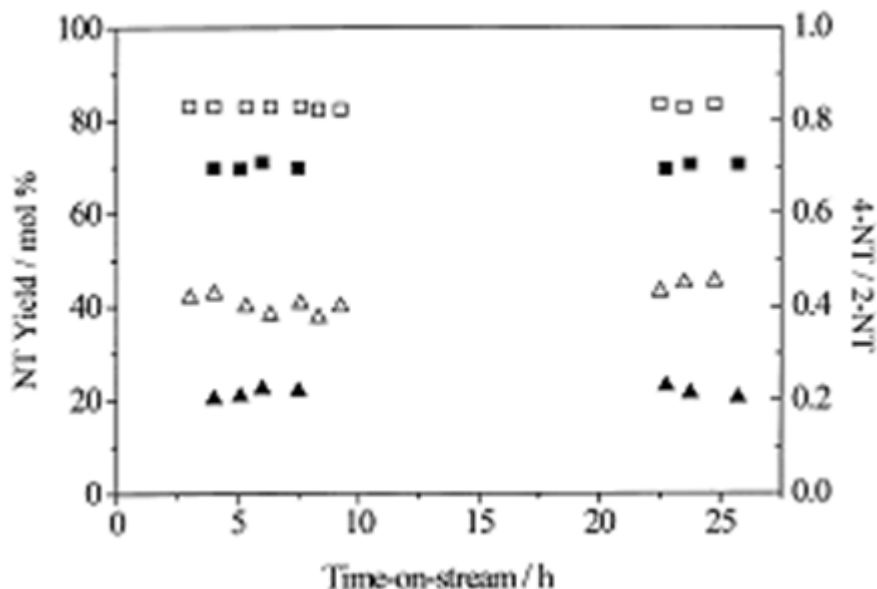
The common nitration method described above has a number of disadvantages; perhaps the most significant being the production of large quantities of spent acid which has to be regenerated because its neutralization and disposal on a large scale is environmentally and economically unsound [14]. Another one is generation of considerable amounts of environmentally harmful waste during the purification of the products [15]. Other disadvantages include the hazards associated with handling the nitrating agent, as well as overnitration [16]. Furthermore, this reaction is not selective, and usually results in a mixture of isomers some of which are less desirable than others. For example, toluene nitration using this method produces a mixture of 55-60% of ortho- or o-NT, 35-40% of para- or p-NT, and 3-4% of meta-, or m-NT [12]. This leads to large quantities of unwanted product because the demand for p-NT is greater than for the other isomers [12, 17]. The conventional techniques used to increase the ratio of p- to o- isomers, such as nitration in the presence of phosphoric acid or in the presence of aromatic sulfonic acids increase the p/o ratio from 0.6 to 1.1-1.5 [12], but require additional use of environmentally harmful reactants. Another challenge associated with this reaction is the formation of oxidative byproducts. The addition of the nitro group to the aromatic ring of toluene strongly activates its methyl group making it susceptible to oxidation. Therefore, industrial nitration of toluene must be carried out at low temperatures to minimize formation of the undesired oxidation products [12]. In a batch process, for example, the acids are added at 25°C and the reaction is carried out at 35 – 40°C [12]. The total NT yield in this reaction is 96% for a batch process, but most patents for continuous processes report yields of up to 50% [12].

### 1.3 Improved Nitration Methods

The disadvantages of the conventional approach to nitration have motivated research aimed at finding cleaner, safer, and more efficient methods. One direction of this research has been to replace liquid sulfuric acid with solid catalysts, which tend to be safer, environmentally friendlier, and easier to separate from the reaction solution than sulfuric acid. In addition, in the case of toluene nitration, surface reaction tends to favor formation of the desirable p-isomer [18].

Vassena, et al., [14] nitrated toluene in vapor phase using fuming nitric acid over solid acid catalysts. Several catalysts were tested, including zeolites and non-zeolitic materials. These can be divided into three groups: zeolites (ZSM-5, ZSM-12, beta and mordenite), non-microporous solid acids – Nafion® and Deloxan® (a polysiloxane bearing alkylsulfonic acid groups of Degussa), and preshaped silicas impregnated with sulfuric acid. The reactions were carried out in a fixed bed reactor at atmospheric pressure and at temperatures ranging from 130 °C to 160 °C.

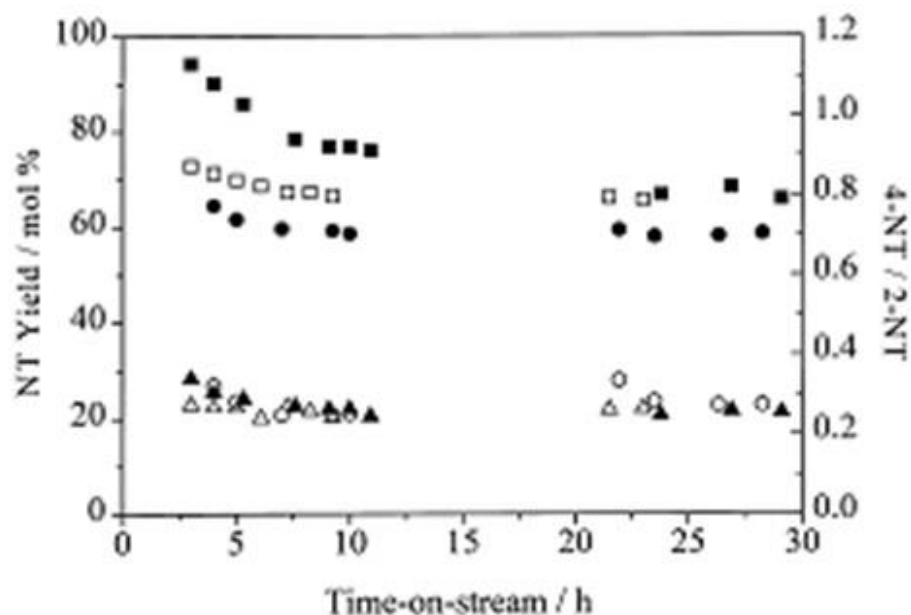
The results of their experiments are shown in Figures 1.1-1.4. As seen from Figure 1.1, NT yield fluctuated around 20% for the reaction carried out without solid acid catalyst and around 40% for Deloxan catalyzed reaction. In both cases, the yield did not increase when the residence time was increased from 4 to 26 hours. Para/ortho ratio was approximately 0.7 for the uncatalyzed reaction and 0.8 for the reaction catalyzed with Deloxan®.



**Figure 1.1** Vapor phase nitration of toluene: blank experiment and nitration with Deloxan. NT yield (left scale):(solid triangles)- without solid acid; (empty triangles) with Deloxan®. P/O ratio (right scale); (solid squares) – without solid acid, (empty squares) with Deloxan® [14].

Source: Vassena D., K.A., Prins R., *Potential routes for the nitration of toluene and nitrotoluene with solid acids*. Catalysis Today, 2000. Vol 60, p. 275-287.

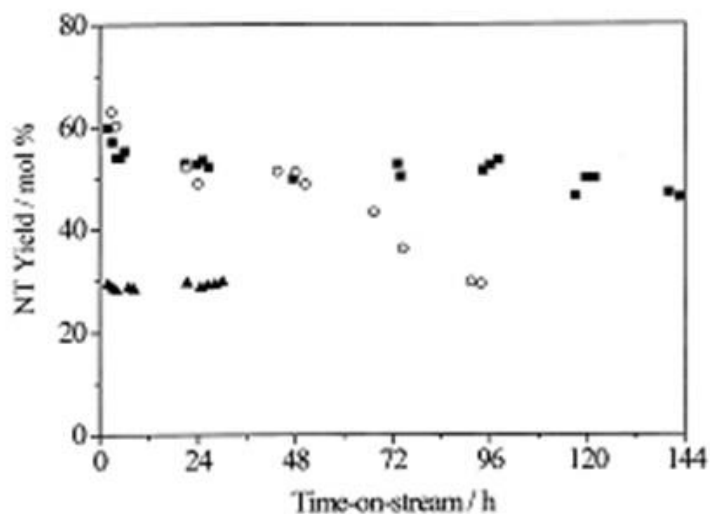
Zeolite catalyzed reaction results are shown in Figure 1.2. As can be seen from the plot, NT yields for the zeolite-catalyzed reaction stayed close to 20%, but the p/o ratio varied from about 0.7 to about 1.1. This indicates that only some zeolites (namely H-beta) actually catalyzed the reaction, causing it to take place on the surface and thus resulting in a higher p/o ratio. Others did not affect the reaction, hence the yield stayed at 20%, same as for the uncatalyzed reaction, and the p/o ratio did not exceed 0.7, indicating a bulk reaction.



**Figure 1.2** Vapor phase nitration of toluene with H-beta, H-ZSM-12 and H-ZSM-5. NT yield (left scale): solid triangle-H-beta; empty triangle - H-ZSM-5; empty circle - H-ZSM-12; P/O ratio (right scale): solid square –H-beta; empty square - H-ZSM-5; solid circle - H-ZSM-12 [14].

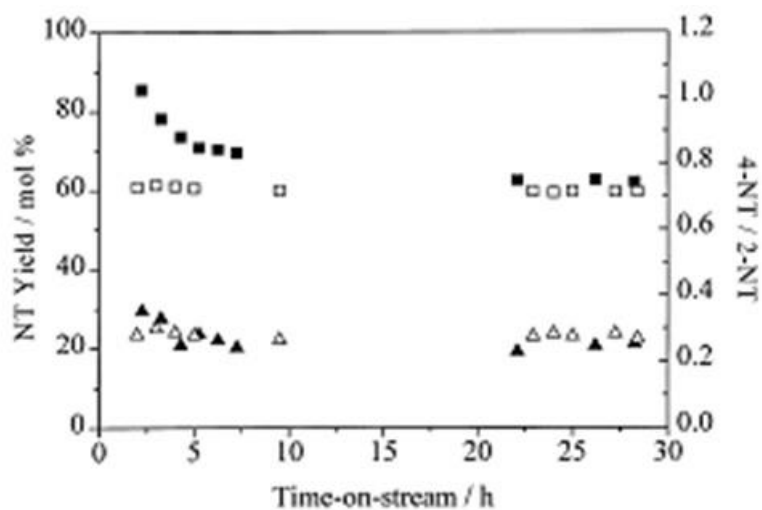
Source: Vassena D., K.A., Prins R., Potential routes for the nitration of toluene and nitrotoluene with solid acids. *Catalysis Today*, 2000. Vol 60, p. 275-287.

Figures 1.3 and 1.4 illustrate the results of toluene nitration over preshaped silica pellets impregnated with  $\text{H}_2\text{SO}_4$  and over mordenite. The former was the only catalyst among those considered that produced NT yields of up to 60%, and even that only when the samples with high content of sulfuric acid were used.



**Figure 1.3** Results of a long-term experiment over preshaped silica impregnated with H<sub>2</sub>SO<sub>4</sub>. NT yield: solid squares - 80% H<sub>2</sub>SO<sub>4</sub>; open circles- 70% H<sub>2</sub>SO<sub>4</sub>; solid triangles – 8% H<sub>2</sub>SO<sub>4</sub> [14].

Source: Vassena D., K.A., Prins R., Potential routes for the nitration of toluene and nitrotoluene with solid acids. Catalysis Today, 2000. Vol 60, p. 275-287.



**Figure 1.4** Vapor phase nitration over mordenite. NT yield (left scale): solid triangles- H-mor(74); open triangles- H-mor(4.6); P/O ratio (right scale): solid squares- H-mor(74); open squares- H-mor(4.6) [14].

Source: Vassena D., K.A., Prins R., Potential routes for the nitration of toluene and nitrotoluene with solid acids. Catalysis Today, 2000. Vol 60, p. 275-287.

The conclusion that can be drawn from their study is that among the catalysts considered, only silica impregnated with large loadings of H<sub>2</sub>SO<sub>4</sub> produced reasonable product yields. Furthermore, while this catalyst does improve p/o isomer ratio, thereby addressing the problem of accumulation of unwanted products, it still requires use of fuming nitric acid as well as significant quantities of concentrated sulfuric acid. The latter, despite being attached to silica, gets used up and cannot be regenerated, as reported in the study. Therefore that approach does little to alleviate the environmental and the safety concerns associated with the traditional nitration methods.

In another study [19], the same group carried out a liquid phase nitration of toluene using 65% nitric acid over sulfuric acid impregnated silica and H-mordenite obtaining mono- and di- nitrotoluenes. High yields for both mono and di nitration were obtained with silica-supported sulfuric acid but the p/o ratio stayed at about 0.7. In addition, water produced as a byproduct had a negative effect on the yield. The reaction conditions and the results are listed in Table 1.1.

**Table 1.1** Conditions and Result of the Liquid Phase Nitration of Toluene

| Nitration of toluene using 50% H <sub>2</sub> SO <sub>4</sub> /SiO <sub>2</sub> <sup>a</sup> |                  |                |              |           |               |                 |
|--|------------------|----------------|--------------|-----------|---------------|-----------------|
| Cat H <sup>+</sup> /HNO <sub>3</sub>   | Temperature (°C) | Conversion (%) | NT Yield (%) | 4-NT/2-NT | DNT Yield (%) | 2,4-DNT/2,6-DNT |
| 3.2  | 25               | 100            | 99.0         | 0.69      | 1.0           | –               |
| 3.2  | 50               | 100            | 96.7         | 0.70      | 3.3           | 3.1             |
| 9.5  | 25               | 100            | 0.0          | –         | 100.0         | 4.0             |
| 9.5 <sup>b</sup>   | 25               | 100            | 0.0          | –         | 100.0         | 3.2             |

<sup>a</sup> Reaction conditions: 3.2–3.8 g catalyst activated in static air at 120°C for 18 h, 65 wt.% HNO<sub>3</sub>, HNO<sub>3</sub>/toluene=2, solvent 10 ml CCl<sub>4</sub>, 24 h reaction time.

<sup>b</sup> Regenerated and reused.

Source: A. Kogelbauer, D.V., R. Prins, J. N. Armor, Solid acids as substitutes for sulfuric acid in the liquid phase nitration of toluene to nitrotoluene and dinitrotoluene. Catalysis Today, 2000. Vol. 55, p. 151-160.

More recently, Gong et al., [20], carried out liquid phase nitration of toluene using dilute nitric acid (50%) over silica supported Cs salt of phosphomolybdic acid

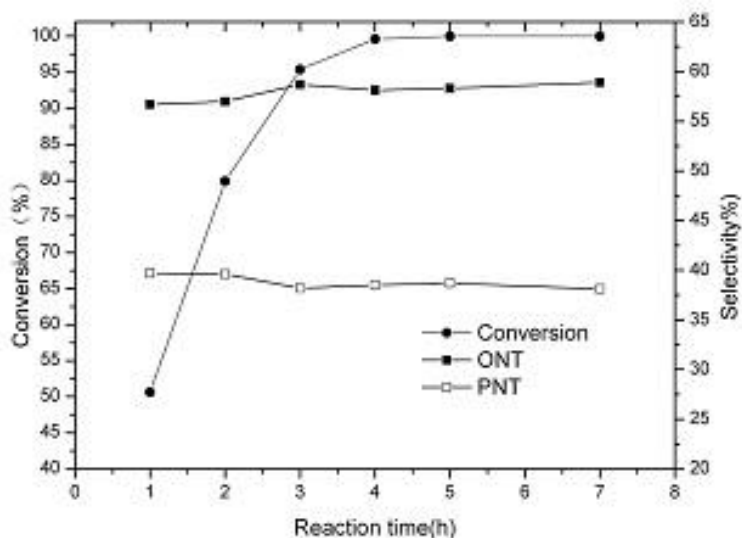
( $\text{Cs}_{2.5}\text{H}_{0.5}\text{PMoO}_{40}$ ) and achieved remarkably high yields of up to 99.6% NT. The reaction was carried out in a stirred batch reactor with the highest product yields achieved at the reaction times of over 4 hrs. It was also found that the catalyst could be easily regenerated and reused. After separation by filtration, washing with distilled water several times and drying at 110 °C, it was reused several times and exhibited almost no drop in catalytic activity. The reaction conditions are summarized in Table 1.2 and the results are shown in Figure 1.5.

**Table 1.2** Reaction Conditions for Toluene Nitration Over  $\text{Cs}_{2.5}\text{H}_{0.5}\text{PMoO}_{40}$  Experiments

| Catalyst                 | BET surface area ( $\text{m}^2/\text{g}$ ) | Pore Volume ( $\text{cc/g}$ ) | $E_i$ (mV) potentiometric titration | Toluene conversion <sup>a</sup> (%) | Selectivity (%) |      |
|--------------------------|--|-------------------------------|-------------------------------------|-------------------------------------|-----------------|------|
|                          |  |                               |                                     |                                     | ONT             | PNT  |
| CsPMA-5/ $\text{SiO}_2$  | 779  | 0.73                          | 161                                 | 77.9                                | 58.8            | 38.3 |
| CsPMA-10/ $\text{SiO}_2$ | 598  | 0.69                          | 358                                 | 95.4                                | 58.7            | 38.2 |
| CsPMA-20/ $\text{SiO}_2$ | 526  | 0.60                          | 375                                 | 99.6                                | 58.1            | 38.6 |
| CsPMA-30/ $\text{SiO}_2$ | 358  | 0.32                          | 219                                 | 93.5                                | 58.3            | 38.5 |

<sup>a</sup> The reaction conditions are the ratio by volume of toluene: Nitric acid is 1:3, the catalyst weight is 0.3 g, and the reaction is carried out at 70 °C under stirring for 3 h.

Source: Gong, S., et al., Stable and eco-friendly solid acids as alternative to sulfuric acid in the liquid phase nitration of toluene. Process Safety and Environmental Protection, 2014. Vol. 92(6): p. 577-582.



**Figure 1.5** Effect of reaction time on the conversion of toluene over CsPMA-10/ $\text{SiO}_2$ .

Source: Gong, S., et al., Stable and eco-friendly solid acids as alternative to sulfuric acid in the liquid phase nitration of toluene. Process Safety and Environmental Protection, 2014. Vol. 92(6): p. 577-582.



This method has clear advantages over the ones discussed previously. It succeeded in eliminating the need for sulfuric acid, and even nitric acid was used in its dilute form offering clear benefits in terms of both safety and environmental impact. Furthermore, converting 99.6% of toluene to NT means that only a small amount of byproducts is generated, thus the need for purification is reduced. At the same time p/o isomer ratio for this method does not exceed 0.66, thus the problem of unwanted product accumulation persists.

In a similar vein, Adamiak et al., [21] achieved high yields of mono- and di-nitrotoluenes by nitrating toluene with fuming nitric acid over  $\text{MoO}_3/\text{SiO}_2$  catalyst modified with  $\text{H}_3\text{PO}_4$ . The characterization of catalyst showed that phosphoric acid reacted with molybdenum oxide forming phosphomolybdic acid, which catalyzed the nitration reaction. Good para- selectivity was observed for this process with p/o ratios greater than 1 and reaching 2.09 in one case.

**Table 1.3** Conditions and Results of Toluene Nitration Using  $\text{H}_3\text{PO}_4$  Modified  $\text{MoO}_3/\text{SiO}_2$  Catalyst

| Amount of $\text{H}_3\text{PO}_4$ , wt.% | TN conversion, wt.% | Composition of product, wt.% |      | Composition of MNT, wt.% |      |      | Ratio p/o |
|--|---------------------|------------------------------|------|--------------------------|------|------|-----------|
|  |                     | MNT                          | DNT  | o-NT                     | m-NT | p-NT |           |
| HPM                                      | 100                 | 89.4                         | 10.6 | 42.6                     | 1.2  | 56.2 | 1.32      |
| HPM <sup>a</sup>                         | 10.5                | 88.5                         | 11.5 | 31.6                     | 2.8  | 65.6 | 2.09      |
| 6.4                                      | 100                 | 98.6                         | 1.4  | 47.1                     | 1.0  | 51.9 | 1.10      |
| 5.7                                      | 100                 | 92.8                         | 7.2  | 43.0                     | 1.3  | 55.7 | 1.30      |
| 5.7 <sup>a</sup>                         | 74.1                | 94.6                         | 5.3  | 44.0                     | 0.7  | 55.3 | 1.26      |
| 5.7 <sup>b</sup>                         | 33.5                | 88.5                         | 11.5 | 47.1                     | 1.3  | 51.6 | 1.10      |
| 1.4                                      | 100                 | 85.0                         | 15.0 | 42.4                     | 0.9  | 56.7 | 1.34      |
| 0 [3]                                    | 92                  | 100.0                        | –    | 48.0                     | 1.7  | 50.3 | 1.05      |
| Without catalyst                         | 5.0                 | 100                          | –    | 51.4                     | 3.1  | 45.5 | 0.88      |

<sup>a</sup> Second reaction using the same catalyst used in the first reaction.

<sup>b</sup> The fifth reaction using the same catalyst as used in the previous reactions.

Source: Adamiak, J., et al., Characterization of a novel solid catalyst,  $\text{H}_3\text{PO}_4/\text{MoO}_3/\text{SiO}_2$ , and its application in toluene nitration. *Journal of Molecular Catalysis A: Chemical*, 2011. Vol. 351, p. 62-69.

These approaches, however, still rely on nitric acid as the nitrating agent, which is a disadvantage in terms of safety and possible corrosion of the equipment. These concerns

have prompted some researchers to consider other sources of nitronium ion. Peng et al., [22] carried out nitration of toluene using liquid NO<sub>2</sub> and molecular oxygen over zeolite catalysts and achieved p/o ratio as high as 14 using HZSM-5. Perves et al., [23] used nitronium tetrafluoroborate as a source of nitronium ion. These methods, however, while achieving promising results, rely on exotic and expensive reactants and/or catalysts. Therefore, they are not currently practical from the industrial standpoint.

## **1.4 Mechanochemically Induced Nitration Reactions**

A new and potentially promising approach to this problem is to carry out the nitration reaction in solid phase using nitrate salts as sources of nitronium ion, with the reaction being driven by mechanical agitation, or mechanochemically. Eliminating solvents and acids offers substantial reduction of the environmental impact of nitration; using inexpensive and readily available nitrogen sources and catalysts offers potential cost benefits as well.

### **1.4.1 Mechanochemical Reactions**

Although the concept of carrying out reactions in solid phase by mechanical agitation, known as mechanochemistry, has existed for centuries, with the earliest references to mechanochemical reactions dating back to 4<sup>th</sup> century BCE, its application has traditionally been limited to insoluble materials [24]. For soluble reactants, on the other hand, the default approach has been to carry out the reactions in solution [25]. Last several decades, however, have witnessed steadily increasing interest toward mechanochemical synthesis, and the manifestation of the versatility and the potential of this approach [26-38]. There are two reasons behind this recent boom in mechanochemical research. First, it is

becoming increasingly clear that this approach can be effective and even advantageous in a wide range of synthesis. Second, there is an increasing awareness that our current dependence on solvents is both wasteful of fossil derived materials, and harmful to the environment; thus it is unsustainable [25].

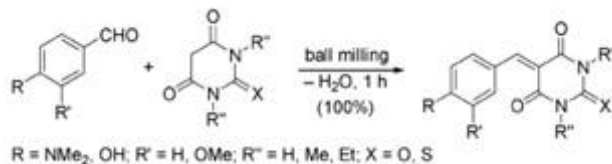
Table 1.4 lists some examples of reactions [25] that have been successfully carried out mechanochemically. This illustrates the versatility of the approach.

**Table 1.4** Examples of Reactions that Have Been Carried Out Mechanochemically

| Reaction                           | Comment  |
|------------------------------------|--|
| Metal halide reduction [39]        | Performed by Michael Faraday in 1820   |
| Alloying [40, 41]                  | One of the original applications, which is still important today. Metals or combinations of metal oxides with reducing agents can be used.   |
| Cocrystallization [42]             | Various types of cocrystals have been synthesized. Liquid assisted grinding often yields best results.   |
| Knoevenagel condensation [43]      | Important C-C bond forming reaction forming $\alpha$ - $\beta$ unsaturated carbonyl compounds. First carried out mechanochemically in by Kaupp in 2003 [43]  |
| Peptide synthesis [44]             | Reducing the amount of solvents is one of the challenges of traditional peptide synthesis that is met by the mechanochemical approach [25].  |
| Fullerene dimerization [45]        | C <sub>120</sub> dumbbell formed in high speed vibration milling   |
| Synthesis of Molecular cages[46]   | Very large covalent organic cages can be assembled by solvent-free ball milling[46]  |
| Coordination polymerization (MOFs) | Ligand addition, ligand exchange, and acid base reactions involving coordination polymers have been carried out using various mechanochemical techniques such as liquid assisted grinding[47], and neat grinding[48] |

A typical Knoevenagel condensation reaction carried out mechanochemically is illustrated in Figure 1.6. Use of stoichiometric amounts of reactants results in quantitative

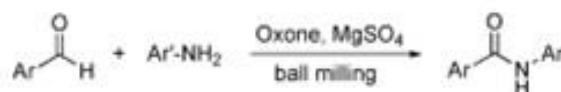
yield of the product. The temperature increase associated with ball milling plays an important role in promoting the reaction [25].



**Figure 1.6** Knoevenagel condensation.

Source: S.L. James, C.J.A., C. Bolm, D. Braga, P. Collier, T. Frišić, F. Grepioni, K.D.M. Harris, G. Hyett, W. Jones, A. Krebs, J. MacK, L. Maini, A.G. Orpen, I.P. Parkin, W.C. Shearouse, J.W. Steed, D.C. Waddell, *Mechanochemistry: Opportunities for new and cleaner synthesis*. Chemical Society Reviews, 2012, Vol: **41**, p. 413-447.

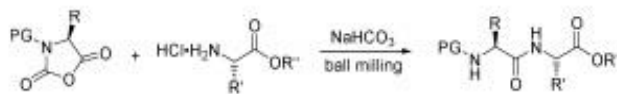
Figure 1.7 shows an example of an amidation reaction. Traditional methods for introduction of the amide group often require expensive transition metal catalysts and/or toxic reactants. This solvent free route for direct amidation of aryl aldehydes with anilines in ball mill overcomes these problems[25].



**Figure 1.7** Direct oxidative amidation

Source: S.L. James, C.J.A., C. Bolm, D. Braga, P. Collier, T. Frišić, F. Grepioni, K.D.M. Harris, G. Hyett, W. Jones, A. Krebs, J. MacK, L. Maini, A.G. Orpen, I.P. Parkin, W.C. Shearouse, J.W. Steed, D.C. Waddell, *Mechanochemistry: Opportunities for new and cleaner synthesis*. Chemical Society Reviews, 2012, Vol: **41**, p. 413-447.

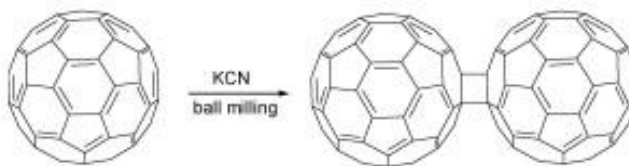
The solvent free peptide synthesis illustrated in Figure 1.8 results in high product yields using simple baking soda as a catalyst [25].



**Figure 1.8** Solvent-free peptide synthesis

Source: S.L. James, C.J.A., C. Bolm, D. Braga, P. Collier, T. Friš, F. Grepioni, K.D.M. Harris, G. Hyett, W. Jones, A. Krebs, J. MacK, L. Maini, A.G. Orpen, I.P. Parkin, W.C. Shearouse, J.W. Steed, D.C. Waddell, *Mechanochemistry: Opportunities for new and cleaner synthesis*. Chemical Society Reviews, 2012, Vol: **41**, p. 413-447.

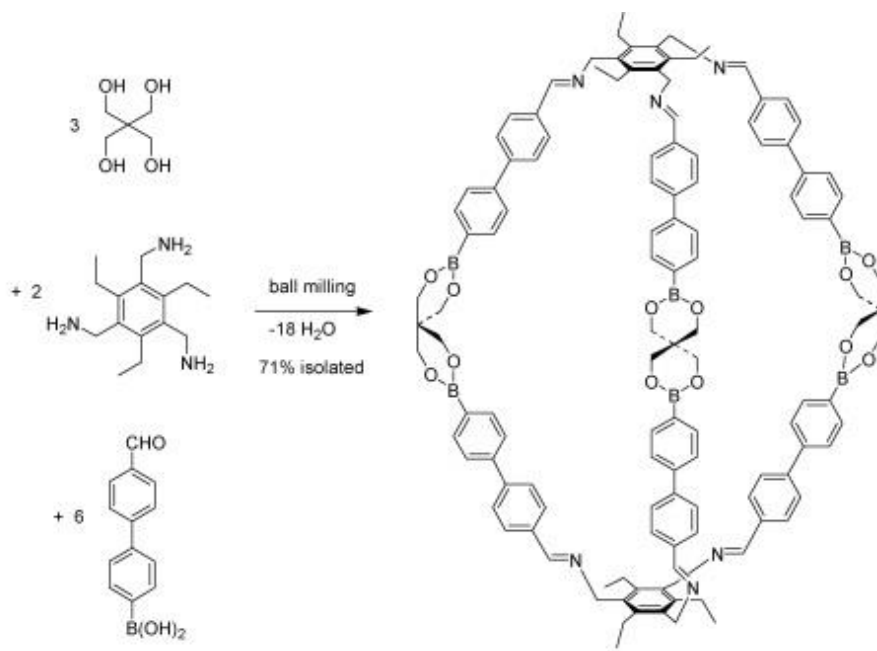
Fullerene dimerization catalyzed by KCN (Figure 1.9) has been carried out by several research groups. Other potassium salts, such as carbonate and acetate also promote the reaction resulting in a mixture of the dimer and the unchanged C<sub>60</sub> in the ratio of 3:7 [45].



**Figure 1.9** Fullerene dimerization

Source: Cheng, X., et al., Solvent-free synthesis of dihydrofuran-fused [60]fullerene derivatives by high-speed vibration milling. Chinese Chemical Letters, 2005, Vol: **16**(10), p. 1327-1329.

Içli et al. [46] synthesized the molecular cage shown in Figure 1.10 in a ball mill with 71% yield. A smaller version of this cage was obtained with 94% yield compared to 24% yield obtained in solution. This reaction involves formation of 18 boronate ester and imine linkages between 11 components.



**Figure 1.10** Solvent-free ball milling synthesis of a large organic cage.

Source: İçli, B., et al., Synthesis of molecular nanostructures by multicomponent condensation reactions in a ball mill. *Journal of the American Chemical Society*, 2009. Vol: **131**(9), p. 3154-3155.

Current understanding of the mechanisms of mechanochemical reactions is still rather deficient. A number of models have been proposed but their application in specific reactions is unclear. It is generally understood that the reactions occur at points of contact between solid surfaces rather than in the bulk of the material, but there are various theories explaining what occurs on these interfaces that causes the reactions to proceed. One possibility is that mechanical impact causes dramatic increase in lattice stress. This stress then relaxes, either physically, by emission of heat, or chemically, by ejection of atoms or electrons, formation of excited states on the surface, bond breakage, and other chemical transformations [49]. This can cause chemical reactions to occur in the field of mechanical stress or even after the stress is removed, by the action of reactive species such as free radicals formed under the action of mechanical stress, that can now cause the reaction to propagate further [49]. Other models discussed in the literature include the “hot-spot”

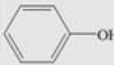

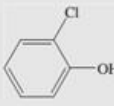
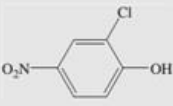


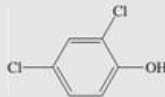
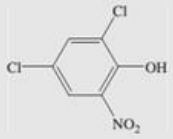
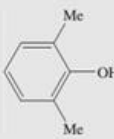
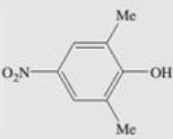
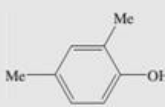
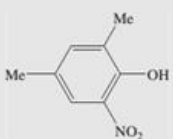
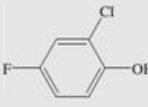
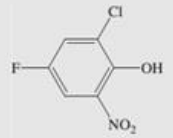
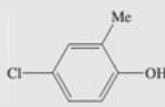
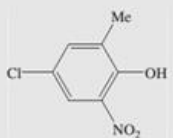
theory and the “magma-plasma model” [50]. According to the former theory, small protuberances on the two surfaces sliding against each other cause plastic deformations associated with dramatic temperature increases. In the brittle materials, such increases can occur at the tips of propagating cracks. It is proposed that local temperatures in such hot spots can reach hundreds or thousands of degrees Celsius for very brief periods. According to the latter model, temperatures of the order of  $10^4$  °C can be generated at impact points. These can cause transient plasmas, and ejection of energetic species including free electrons [25]. It is not likely, however, that such high temperatures occur to a significant extent in organic reactions because if they did, they would cause decomposition of many species [25]. Instead, covalent bond forming organic reactions have been suggested to occur through the formation of intermediate liquid eutectic phases [25]. There has been little study on the application of these mechanisms to specific reactions, despite the fact that the parameters affecting the process can depend significantly on the specific mechanism. Lowering temperature, for example, usually improves the effectiveness of milling processes, and can improve the rate of reactions caused by formation of surface defects. If, however, the reaction proceeds through the formation of a localized liquid phase, its rate is likely to drop when the temperature is lowered.

#### **1.4.2 Mechanochemical Nitration of Organic Compounds**

Despite the wide variety of reactions that have been carried out mechanochemically to date, nitration of aromatics has been largely overlooked. An exception is the work of Albadi et al. [6] where a number of aromatic compounds were nitrated in a mortar using sodium nitrate in the presence of melamine trisulfonic acid (MTSA) as a source of the nitronium ion. The reaction times ranged from 5 to 60 minutes and the nitrated products were

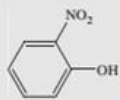
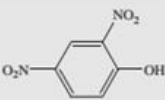
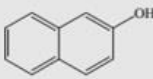
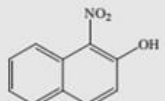
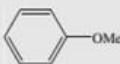

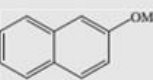
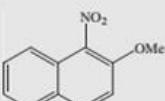

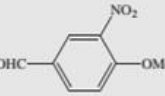

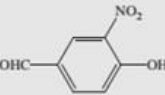
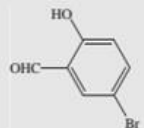
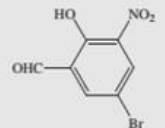
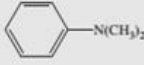
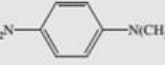
obtained with high yields. Table 1.5 lists the aromatic compounds successfully nitrated in their study.

**Table 1.5** List of Aromatic Compounds Nitrated by Albadi, et al. [6] (Continued)

| Entry | Substrate   | Product   | Time (min) | Yield (%) <sup>a</sup> |
|-------|---|---|------------|------------------------|
| 1     |    |    | 5          | 87                     |
| 2     |    |    | 12         | 88                     |
| 3     |    |    | 30         | 86                     |
| 4     |    |   | 55         | 87                     |
| 5     |  |  | 5          | 89                     |
| 6     |  |  | 30         | 87                     |
| 7     |  |  | 22         | 89                     |
| 8     |  |  | 18         | 87                     |



**Table 1.5** (Continued) List of Aromatic Compounds Nitrated by Albadi, et al. [6]

| Entry | Substrate   | Product   | Time (min) | Yield (%) <sup>a</sup> |
|-------|---|---|------------|------------------------|
| 9     |    |    | 30         | 88                     |
| 10    |    |    | 60         | 82                     |
| 11    |    |    | 15         | 88                     |
| 12    |    |    | 60         | 75                     |
| 13    |    |    | 45         | 82                     |
| 14    |   |   | 32         | 85                     |
| 15    |  |  | 30         | 87                     |
| 16    |  |  | 5          | 86                     |

<sup>a</sup> Isolated yield.

Source: Jalal Albadi, F.S., Bahareh Ghabezi, Tayebah Seiadatnasab, Melamine trisulfonic acid catalyzed regioselective nitration of aromatic compounds with sodium nitrate under solvent-free conditions. *Arabian Journal of Chemistry*, 2012. Vol: **10**, p. S509-S513

It is worth pointing out, however, that all the compounds nitrated in that study were activated by strongly electron donating substituents such as the –OH, –OMe, or –N(CH<sub>3</sub>)<sub>2</sub> groups. Nitration of toluene, whose methyl group is less activating in an electrophilic substitution reaction than the above listed groups, was not reported in that article.

In this study, we take the approach of mechanochemical nitration using nitrates a step further by applying environmentally benign catalysts, such as  $\text{MoO}_3$  or combinations of  $\text{MoO}_3$  and  $\text{SiO}_2$  to nitrate toluene in a ball mill. Unlike MTSA, unmilled  $\text{MoO}_3$  is not an acid, but under the vigorous mechanical impacts of the ball milling process, it has been found (see Chapter 2) to acquire acidic properties allowing it to catalyze the formation of nitronium ion from sodium nitrate.

The catalytic activity of  $\text{MoO}_3$ , particularly in hydrocarbon oxidation reactions has long been known, and many studies have been performed examining its use in partial oxidation of methanol [51, 52] and other compounds [51]. Although the mechanism of these reactions is subject to much debate in the literature [51], there is evidence, based on atomic force microscopy studies performed by Smith and Rohrer [53], that the uncoordinated  $\text{Mo}^{6+}$  cations on step edges and defects are the active sites for oxidation of alcohols. These electrophilic cations also possess Lewis acid properties, and therefore can catalyze formation of the nitronium ion from the nitrate. Thus the ball milling process, which breaks the crystals forming many new defects can be used to greatly enhance the Lewis acid properties of  $\text{MoO}_3$  making it an effective catalyst in mechanochemical aromatic nitration reactions.

## CHAPTER 2

### MECHANOCHEMICAL NITRATION OF TOLUENE: FEASIBILITY<sup>1</sup>

#### 2.1 Introduction

Nitration of aromatic compounds is a common reaction used for preparation of multiple organic energetic materials, including TNT, NTO, and others[54-56]. The reaction is an electrophilic aromatic substitution; its practical implementations typically involve multiple liquid reagents. An important case is the nitration of toluene with mixed acids: nitric acid/sulfuric acid, nitric acid/aromatic sulfonic acid or nitric acid/phosphoric acid[57]. While the technology is well established, it is associated with a number of environmental and safety concerns[58]. Most significantly, it generates red water from the sulfiting process for removing unsymmetrical trinitrotoluene isomers [15]. Such concerns stimulate active research on remediation of the red water and other waste generated by nitration of organic compounds on the industrial scale, e.g., see most recent papers [59-62]. New safe and environmentally friendly manufacturing approaches are being actively explored[63, 64]. In one example, recently implemented in a commercial process, an environmentally friendlier method of manufacturing TNT was developed at Radford Army Ammunition Plant operated by ATK [65]. The process involves replacing toluene as a starting material with ortho-mononitrotoluene. Using a nitro compound as a precursor streamlines the following operation; however, ortho-mononitrotoluene needs to be prepared elsewhere, and the associated environmental waste-related issues are being locally bypassed rather than completely solved.

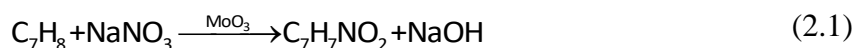
---

<sup>1</sup> Journal Article published in Journal of Energetic Materials, July 2017

Recently, ideas of mechanochemical synthesis originally developed for metal-based materials and inorganic composites have been extended to include synthesis and modification of various organic compounds [25, 66-69]. Although this technology consumes substantial energy, it is readily scalable. It also offers the possibility to eliminate solvents from the process, which has been a significant incentive for its exploration. It is currently considered for preparation of a broad range of organic and inorganic materials, composites, and structures. This work explores the feasibility of mechanochemical processing for nitration of aromatic compounds. If successful, this technology can be developed into an environmentally friendly, solvent free manufacturing method for a wide range of energetic materials or their precursors.

The nitrate source of in this study is sodium nitrate, a readily available, environmentally benign solid. The concept of using sodium nitrate in the presence of an acid as a nitrating agent is not new. However, much more aggressive Lewis acids, e.g.,  $\text{AlCl}_3$ , are used commonly. Working with such materials and disposing of the related chlorinated byproducts is still undesirable. Qian et al. performed nitration of phenols in solvent free conditions using metal nitrates in the presence of oxalic acid as the nitrating agent.[70] Oxalic acid, too, however, is a relatively strong acid; in addition, his work was only with phenols, which are strongly activated towards electrophilic aromatic substitution. Therefore, in this work, molybdenum trioxide,  $\text{MoO}_3$ , which has Lewis acid surface sites, was explored as potential catalyst for nitration. This oxide has long been known for its catalytic properties in a number of reactions including nitration of aromatic compounds. Skupinski et al., for example, used  $\text{MoO}_3/\text{SiO}_2$  to obtain high yields of mononitrotoluene by nitration of toluene with 65% nitric acid[71]. Kemdeo et al. studied the use of  $\text{MoO}_3/(\text{TiO}_2/\text{SiO}_2)$  in nitration of phenol[72], and  $\text{MoO}_3/(\text{SiO}_2\text{-ZrO}_2)$  in nitration of

toluene[73]. Adamiak et al. explored the mechanism of toluene nitration over MoO<sub>3</sub>-SiO<sub>2</sub>[74], and in another study enhanced this catalyst by addition of H<sub>3</sub>PO<sub>4</sub> with excellent results[21]. In all of these studies, however, MoO<sub>3</sub> was used in combination with other metal oxides, and its function was to enhance the acidity of the Bronsted sites present on the surface of silica, titania or zirconia. In the last case it reacted with phosphoric acid to form phosphomolibdic acid – one of the strongest inorganic acids known. These Bronstead acids protonated HNO<sub>3</sub>, leading to formation of nitronium ions, instead of H<sub>2</sub>SO<sub>4</sub> normally used for this purpose. In this study, on the other hand, MoO<sub>3</sub> was used without any support and the source of nitronium ion was NaNO<sub>3</sub> rather than nitric acid – a much more environmentally friendly and easy to handle alternative. These solid reactants, sodium nitrate, NaNO<sub>3</sub>, as a source of the nitro-group and molybdenum trioxide, MoO<sub>3</sub>, as a Lewis acid catalyst, were ball-milled with toluene in order to produce the reaction:



The objective is to demonstrate the feasibility of mechanochemical nitration of toluene using environmentally benign reagents, and to explore how process parameters affect product yield and selectivity.

## 2.2 Experimental

Nitration of toluene was achieved using mechanical milling of toluene, sodium nitrate, and molybdenum oxide as a catalyst. Materials used in the experiments were toluene (Chempure, 99.99 %), molybdenum oxide,  $\text{MoO}_3$  (Alfa-Aesar, 99.95 %), and sodium nitrate (Alfa Aesar, 99%). Ethyl acetate (Alfa Aesar, 99.5 %) was used to extract the reaction products for analysis. Two ball mills were used. A Spex Certiprep 8000D shaker mill (SM) was used for samples of up to 6 g, and a Retsch PM 400MA planetary mill (PM) was used for larger samples of up to 50 g. In both cases, hardened steel vials were used and 9.5 mm (3/8") hardened steel balls served as milling media. Steel balls with 3.2 mm (1/8") diameter were used in one experiment.

Preliminary experiments established the feasibility of mechanochemical formation of ortho- and para-mononitrotoluene, although at low yields. All subsequent experiments were performed in an effort to determine parameters affecting the mononitrotoluene yield and selectivity. The parameters varied were the ball-to-powder mass ratio (BPR) and the relative proportions of the starting reagents.

Table 2.1 summarizes these milling conditions for a set of runs with milling duration of 2 hours. Longer milling times were used in several runs, which are discussed separately. Table 2.1 also shows symbols used to represent the results of different milling runs in subsequent figures. A visual representation of the various charge compositions is given in Figure 2.1 in the form of a ternary compositional diagram.

For most runs, the mole fraction of toluene is relatively low, varying from 6.3 to 4.4 %, as represented by points lined along the  $\text{MoO}_3$ - $\text{NaNO}_3$  axis. The  $\text{MoO}_3/\text{NaNO}_3$  ratio varies in a broad range, and several points are available with substantially varied

toluene/solid ratios. Along with Table 2.1, Figure 2.1 should be used to interpret the experimental results discussed below. Note that some of the points, e.g., filled and open stars, overlap in Figure 2.1.

The milling runs are divided into several groups. In the largest group, milled in the shaker mill and represented by open squares, the relative amounts of  $\text{NaNO}_3$  and  $\text{MoO}_3$  were varied, the amount of toluene was fixed at 0.25 mL, and the total mass of solids was fixed at 5 g. The crossed open circle represents an experiment from the same set, with the  $\text{MoO}_3$  to  $\text{NaNO}_3$  molar ratio of 2.95, identical to one of the hollow squares, except in this case toluene was added after 95 minutes, 25 min before the end of the milling process.

Open and filled triangles represent two experiments in which the amounts of all reactants were doubled (10g of solids and 0.50 ml of toluene) thereby lowering the BPR to 5. The mole ratios of  $\text{MoO}_3$  to  $\text{NaNO}_3$  were 2.94 (filled triangle) and 3.54 (open triangle).



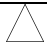






Filled circles and diamonds represent experiments examining the effect of increasing amounts of toluene. The  $\text{MoO}_3$  to  $\text{NaNO}_3$  mole ratio is 1.47 for the circle, and 5.96 for the diamond. In both cases, the toluene amount was increased to 1 ml while maintaining the total mass of solids at 5 g.

The half-filled circles represent runs in which the amount of  $\text{NaNO}_3$  was increased without changing the amounts of  $\text{MoO}_3$  (4.17 g, as in the experiment represented by an open, crossed circle) and toluene (0.25 ml), thus raising the total mass of solids. The mass of  $\text{NaNO}_3$  was doubled from 0.83 to 1.66 g.

The asterisk represents an early experiment with a much higher toluene/solids mass ratio. It used 1.1 ml of toluene and a total of 1.7 g of solids.

The stars represent two planetary mill runs with different milling ball sizes. In these runs, the toluene/solid ratio could be reduced further, while using a well-defined 0.5-ml volume of toluene.

**Table 2.1** Summary of the Milling Conditions for 2 Hr. Runs

| Symbol  | Mill | Ball diam., mm | BPR | Solid mass, g | Molar ratios                        |                           |                            | Mass ratio    |
|---|------|----------------|-----|---------------|-------------------------------------|---------------------------|----------------------------|---------------|
|   |      |                |     |               | MoO <sub>3</sub> /NaNO <sub>3</sub> | MoO <sub>3</sub> /toluene | NaNO <sub>3</sub> /toluene | Toluene/solid |
|    | SM   | 9.5            | 10  | 5             | 0.296-28.92                         | 4.91-14.39                | 0.995-16.57                | 0.043         |
|    | SM   | 9.5            | 5   | 10            | 2.94                                | 12.2                      | 4.15                       | 0.043         |
|   | SM   | 9.5            | 5   | 10            | 3.54                                | 12.6                      | 3.55                       | 0.043         |
|  | SM   | 9.5            | 10  | 5             | 1.47                                | 2.62                      | 1.78                       | 0.174         |
|  | SM   | 9.5            | 8.6 | 5.85          | 1.48                                | 12.24                     | 8.29                       | 0.037         |
|  | SM   | 9.5            | 10  | 5             | 5.96                                | 3.34                      | 0.559                      | 0.174         |
|  | SM   | 9.5            | 10  | 1.76          | 0.98                                | 0.708                     | 0.72                       | 0.564         |
|  | PM   | 9.5            | 3   | 43.3          | 14.75                               | 61.2                      | 4.15                       | 0.010         |
|  | PM   | 3.2            | 3   | 43.3          | 14.75                               | 61.2                      | 4.15                       | 0.010         |

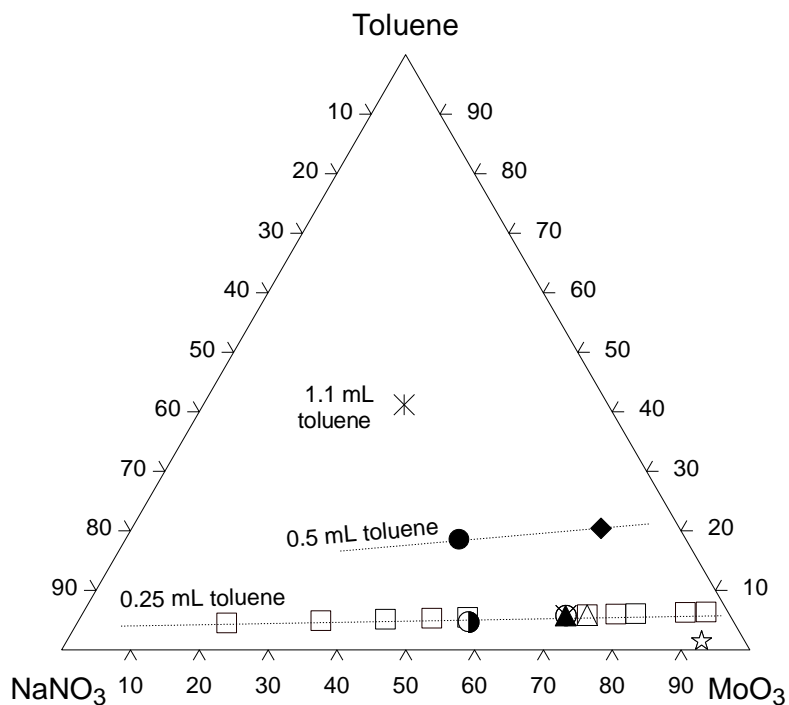
\*Toluene was added 25 minutes before the end of the run.

In addition to the experiments summarized in Table 1, a limited number of experiments were conducted at longer milling times. Specifically, charge compositions with MoO<sub>3</sub>/NaNO<sub>3</sub> ratios of 2.95 and 1.47, milled with 0.25 mL of toluene were milled for 4, 6, and 8 hours.



After milling, the materials were extracted with ethyl acetate, separated from the solid inorganic fraction *by settling* and analyzed in a HP 6890 gas chromatographer (heating profile: 40 °C to 300 °C at 5 K/min) coupled with HP G2350A mass spectrometer. Product species were identified using the NIST Mass Spectral Library (NIST 08), and relative concentrations were determined using GC peak integration. To quantify the results in terms of yield and selectivity, five major byproducts were selected: benzaldehyde, 2,2'-dimethyl-biphenyl, 1-methyl-4-phenylmethyl benzene, 2-methylphenyl-phenylmethanone, and 4-methylphenyl-phenylmethanone. The mononitrotoluene yield was estimated by evaluating the ratio of the sum of all peak areas of mononitrotoluene to the sum of the areas of peaks of toluene and of the above byproducts. The undesired byproduct yield was calculated similarly, and the selectivity was calculated as the ratio of mononitrotoluene yield to the byproduct yield. Effectively, it was the ratio of the areas of all mononitrotoluene peaks to the area of peaks of all the byproducts. Peak areas for all mononitrotoluene isomers were combined for both yield and selectivity assessments.

The specific surface area of MoO<sub>3</sub> was measured before and after milling with NaNO<sub>3</sub> and toluene via *single*-point BET nitrogen adsorption, using a Horiba SA-9600 surface area analyzer. The specimens were outgassed in the instrument cell in a stream of dry N<sub>2</sub> at 150 °C for three hours prior to the measurement. The measurements were run in duplicates.



**Figure 2.1** Ternary diagram showing relative amounts of the reactants in the 2 hr milling experiments.

## 2.3 Results

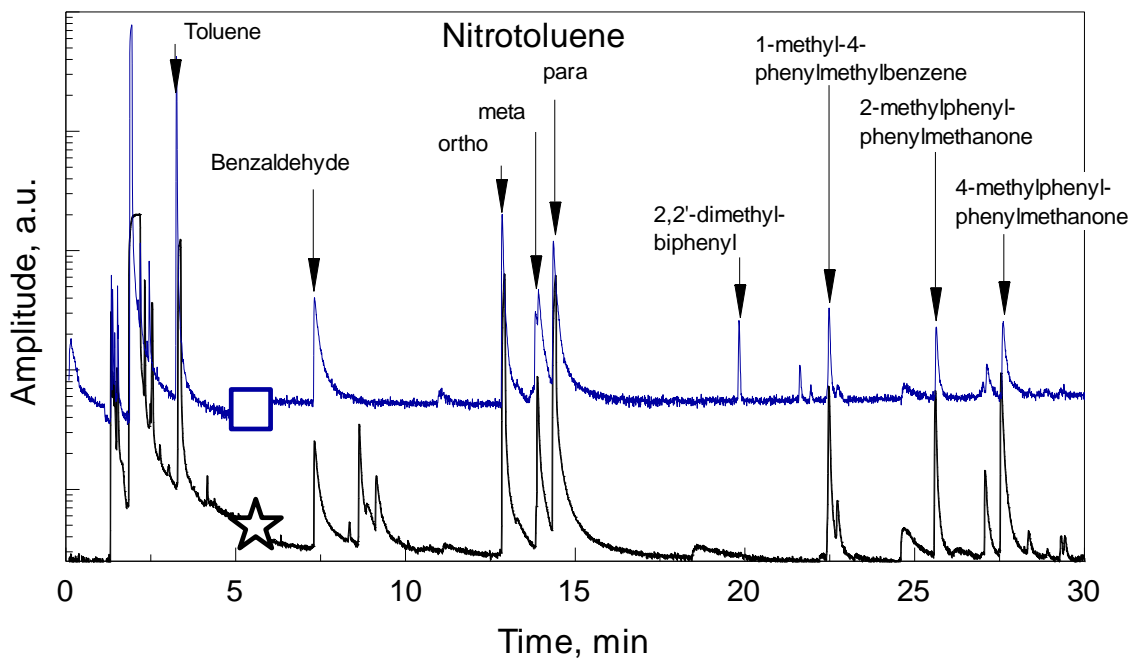
### 2.3.1 Formation of Mononitrotoluene With $\text{MoO}_3$ As A Catalyst

In preliminary, exploratory experiments, toluene and sodium nitrate were milled with several metal oxides with Lewis acid surface sites. These included  $\text{WO}_3$ ,  $\text{TiO}_2$ ,  $\text{Al}_2\text{O}_3$  and  $\text{ZrO}_2$ . Nitration was not observed, and therefore, these materials were not further investigated.

Toluene was successfully nitrated by milling it with  $\text{NaNO}_3$  and  $\text{MoO}_3$ . Characteristic GC-MS traces are shown in Figure 2.2. The top and bottom traces represent 2-hr SM and PM runs, respectively. Each trace is labeled with the symbol representing the run in Table 2.1. For the SM run, the specific mole ratios of the reactants were:  $\text{MoO}_3/\text{NaNO}_3=3.6$ ;  $\text{NaNO}_3/\text{Toluene}=3.53$ . In Figure 2.2, the peaks on the left of the

toluene peaks represent ethyl acetate and are not labeled. In both cases, mononitrotoluene is present as a mixture of isomers. In addition, a number of undesired byproducts are also observed, such as toluene dimers, benzaldehyde, and benzoic acid among others.

The toluene peak on the bottom trace, corresponding to the PM experiment, is very narrow. Most of toluene was converted to either mononitrotoluene or the byproducts. Yield exceeding 40% of nitrotoluene was attained in this PM run with a relatively short milling time of 2 hours. In addition to a high yield, the selectivity of mononitrotoluene production also improved, with substantially greater ratio of the area of the mononitrotoluene peaks to those of other products (benzaldehyde, 1-methyl-4-phenylmethylbenzene, etc.) This clearly shows that the mechanochemical approach offers a feasible way of nitrating toluene with no harmful chemicals and byproducts.



**Figure 2.2** GCMS traces for selected mechanochemical experiments on nitration of toluene. Top: SM; bottom: PM. The mononitrotoluene yield and selectivity respectively are 18.2% and 2.7 for the top, and 42.2% and 4.97 for the bottom traces.

### 2.3.2 Parameters Affecting Product Yield

Figures 2.3 – 2.5 show yield and selectivity of mononitrotoluene production as a function of molar ratios of different materials used in the milling runs. The symbols used in all figures are the same as those shown in Table 2.1. To simplify the interpretation of these results, only 2-hour milling runs are included in this set of plots. Data for both yield and selectivity appear to produce peaks in each of the shown plots.

In most cases, the yield and selectivity correlate with each other. All points with particularly low yields: asterisk, filled circle, and diamond, (except for one open square), correspond to relatively large amounts of toluene used; cf. Table 2.1 and Figure 2.1; these points are shifted to the left in Figure 2.5, because of the low  $\text{MoO}_3$ /toluene ratios. The only exception where a low yield is observed for a relatively small amount of toluene is an open square point (appearing in all Figures 2.3 – 2.5) with the very low concentration of  $\text{NaNO}_3$ , for which the composition is shown at the left bottom corner in Figure 2.1. Conversely, the experiments performed using the PM, for which the ratio of  $\text{MoO}_3$  to toluene was particularly high (points are shifted to the right in Figure 2.5), produced higher yields than the SM experiments with the same ratios of  $\text{NaNO}_3/\text{MoO}_3$  and  $\text{NaNO}_3$ /toluene.

For the same toluene to solid mass ratio of 0.43, the data for both yield and selectivity form relatively clear peaks in both Figures 2.3 and 2.4. In Figure 2.3, the peak is relatively broad and is located at the range of  $\text{NaNO}_3$ /toluene ratios of 1 – 4. In Figure 2.4, the peak corresponds to the  $\text{MoO}_3/\text{NaNO}_3$  ratios of 3 – 15.

Data points in Figure 2.5 form a highly asymmetric peak, with a sharply falling right edge. This peak structure can be understood considering that the same points, for which the toluene/ $\text{MoO}_3$  ratio becomes large, have a much reduced amount of  $\text{NaNO}_3$

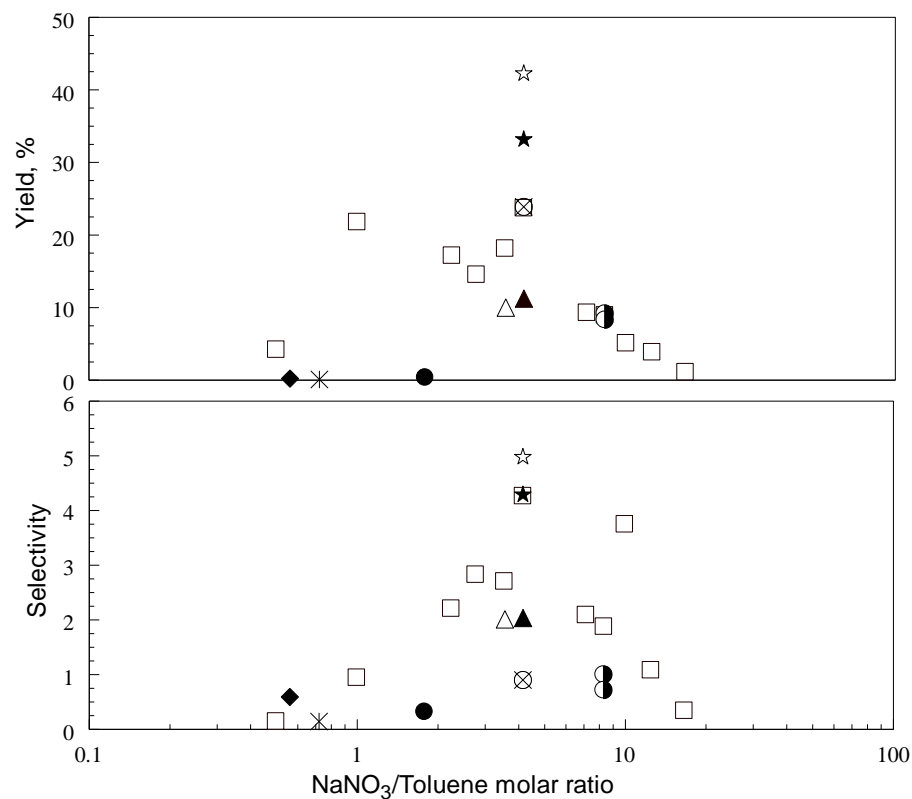
(because the total mass of solid remains fixed at 5 g, see Table 2.1.) Thus, the effect is simply associated with the  $\text{NaNO}_3$  deficiency, which is not explicitly seen from Figure 2.5.

The yield for the run represented by a crossed circle, for which milling was initially dry and toluene was added later in the process coincides with that of the similar run, where toluene was loaded to the milling vial from the very beginning. However, the selectivity represented by the crossed circle run is lower, suggesting that more byproducts formed.

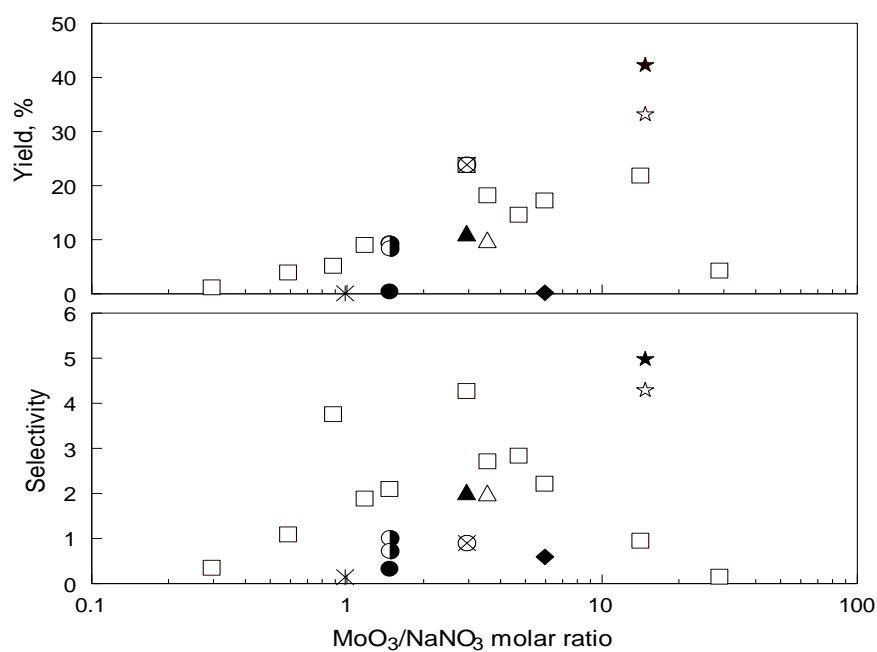
The yield for data points represented by half-filled circles fits well with the trend formed by open squares, suggesting that the increase in the concentration of  $\text{NaNO}_3$  did not change the yield. The selectivity for the half-filled circles was reduced compared to that shown by the open squares.

The data points represented by triangles correspond to a reduced BPR and thus reduced milling dose, which is a measure of the specific energy transferred to the material from the milling tools. These data show a reduced yield compared to the runs represented by open squares and corresponding to a greater milling dose. In qualitative agreement with this observation, for PM runs, the yield is higher for the run represented by an open star, for which larger size balls were used. Although the BPR was the same for both PM runs, larger size balls result in greater impact energies transferred to the material being milled.

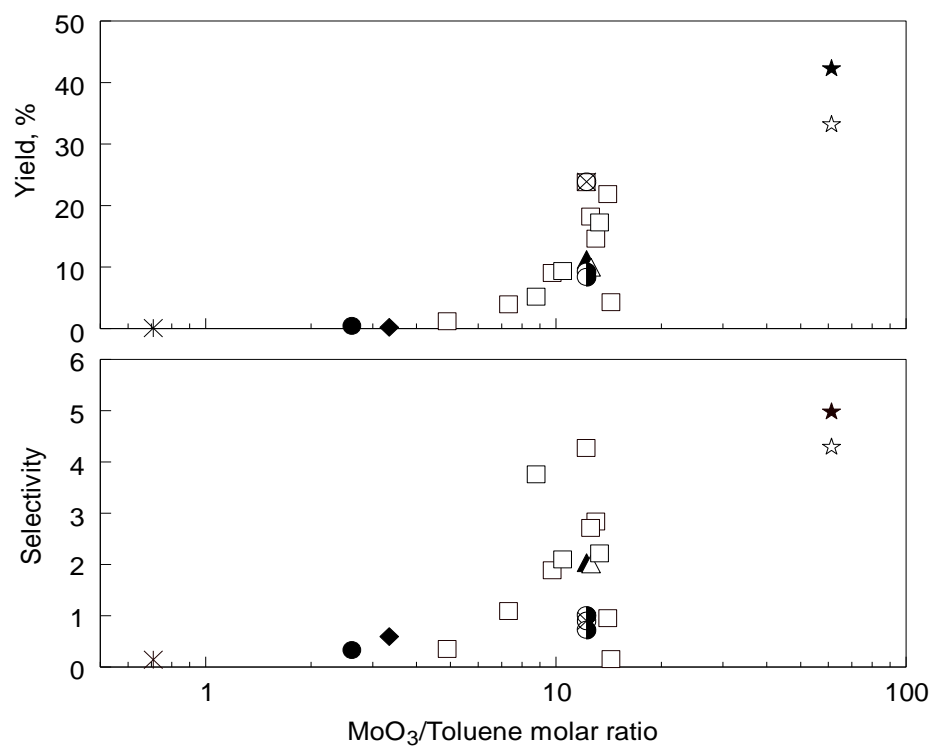
The data points characterizing yield appear to be slightly less scattered than the corresponding data on selectivity. This could simply indicate that the selectivity assessment was prone to more errors.



**Figure 2.3** Mononitrotoluene yield and selectivity vs.  $\text{NaNO}_3$ /toluene molar ratio. Milling time is 2 h.

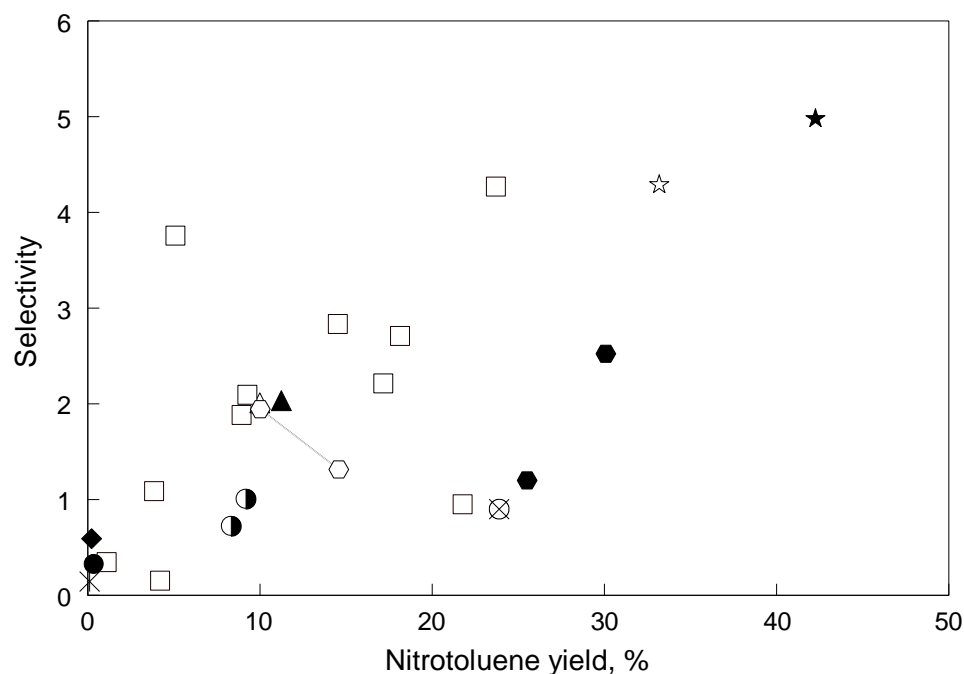


**Figure 2.4** Mononitrotoluene yield and selectivity vs.  $\text{MoO}_3/\text{NaNO}_3$  molar ratio. Milling time is 2 h.



**Figure 2.5** Mononitrotoluene yield and selectivity vs.  $\text{MoO}_3/\text{toluene}$  molar ratio. Milling time is 2 h.

A correlation between the yield and selectivity is well observed from Figure 6, where these values are plotted against each other. This correlation is important, as suggesting that further optimization of the mechanochemical nitration of toluene is likely to generate a cleaner product.

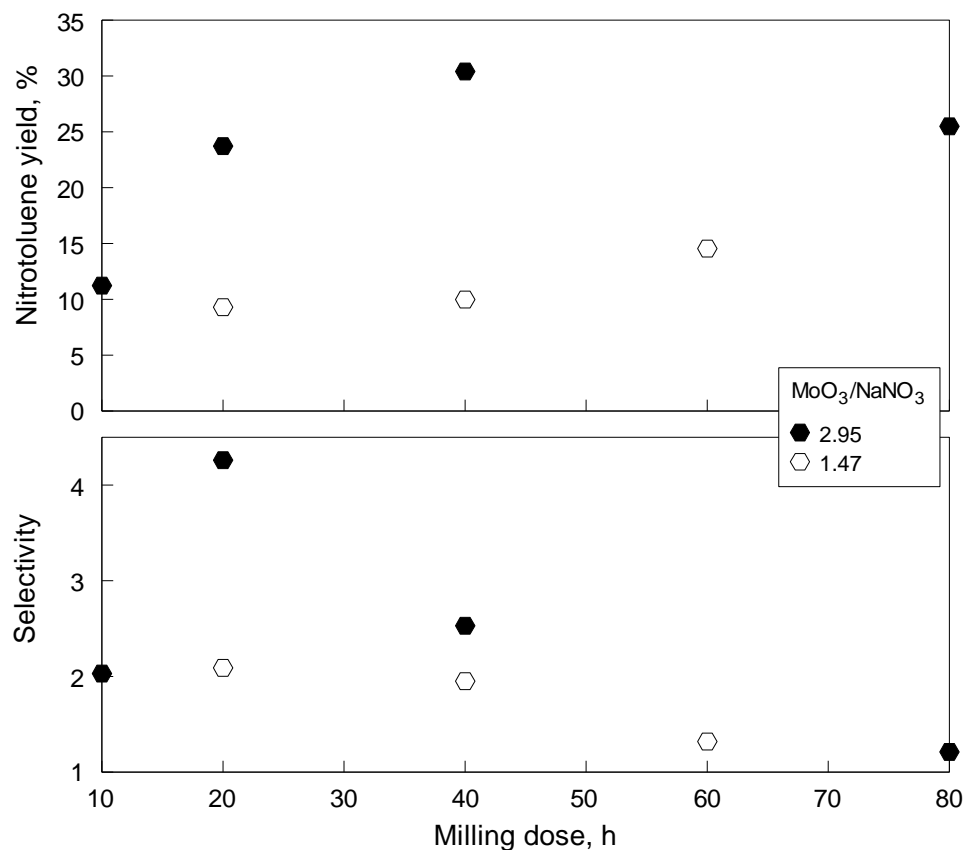


**Figure 2.6** Selectivity vs. mononitrotoluene yield. Symbols for 2-h runs are as shown in Table 2.1. Filled and open hexagons show points, for which the milling dose was varied. Additional details are given in Figure 2.7.

The effect of milling dose on yield and selectivity of the toluene nitration is illustrated in Figure 2.7. For this simplified analysis, the milling dose was estimated as a product of BPR and milling time. Such an estimate can be used to compare runs with the same ball size and performed using the same mill [75-77]. The data in Figure 2.7 include two subsets of SM experiments with  $\text{MoO}_3/\text{NaNO}_3$  ratios of 2.95 and 1.47. The variation of both milling times and BPR affected the milling dose. It is apparent that the increasing milling dose leads to a greater yield; although a saturation seems to occur, especially for the experiments with the  $\text{MoO}_3/\text{NaNO}_3$  ratio of 2.95. It is also apparent that unlike results shown in Figures 2.3 – 2.5, an increase in yield due to a greater milling dose may reduce selectivity, which is an undesirable effect. Additional experiments varying milling dose are needed, in particular, with lower amounts of toluene, observed to increase the



mononitrotoluene yield, to observe the practical maximum achievable for both yield and selectivity.



**Figure 2.7** Mononitrotoluene yield and selectivity vs. milling dose. The point at milling dose of 10 h corresponds to a 2-h milling run with BPR 5, for other points, BPR was 10 and the milling time varied between 2 and 8 h.

To establish the development of the  $\text{MoO}_3$  surface, the location of catalytic Lewis acid sites, as it is being milled, several  $\text{MoO}_3$  samples were prepared using various milling conditions and their surface areas were measured using BET. All samples contained 4.167 g of  $\text{MoO}_3$  loaded in a SM vial with 10-mm balls. The BPR was fixed at 10. The milling time was set to 2 hours. Amounts of toluene added in each experiment varied. Results are shown in Table 2.2. Milling increases surface area markedly, and milling in the presence

of toluene increases the surface area more than milling without toluene. However, varying the amount of toluene does not seem to affect the surface area of MoO<sub>3</sub>.

**Table 2.2** Specific Surface Area For Unmilled And Milled MoO<sub>3</sub> Samples. Results Reflect Two Repeat Measurements

| Material  | Volume of toluene, ml | Surface area, m <sup>2</sup> /g |
|---|-----------------------|---------------------------------|
| initial MoO <sub>3</sub>  | 0                     | 0.23 ± 0                        |
| MoO <sub>3</sub> milled for 2 h with<br>MoO <sub>3</sub> /NaNO <sub>3</sub> of 2.96 | 0                     | 3.14 ± 0.07                     |
|   | 0.25                  | 20.2 ± 0.5                      |
|   | 0.50                  | 19.6 ± 0.1                      |
|   | 0.75                  | 19.7 ± 0.8                      |

## 2.4 Discussion

A higher yield of nitrated products is observed for the NaNO<sub>3</sub>/Toluene molar ratio in the range of 1 – 4 (Figure 2.3). Of the experiments performed with 0.25 mL toluene in the shaker mill (open squares), the highest yield is observed near the stoichiometric NaNO<sub>3</sub>/toluene molar ratio of 1. Almost no yield is observed for higher amounts of toluene (filled circle, diamond, and asterisk), while the highest yield was observed for a much lower toluene/solids ratio in the planetary mill (open star). This suggests that the reaction is limited by the available catalytic surface sites, and providing excess toluene does not result in greater degree of nitration. This is further illustrated in Figure 2.5 showing the observed yield vs. the MoO<sub>3</sub>/toluene ratio. This ratio did not affect the specific surface area of MoO<sub>3</sub> (cf. Table 2.2) suggesting that the number of active sites on the MoO<sub>3</sub> surface did not change. Instead, the change in yield as a function of the MoO<sub>3</sub>/toluene ratio was likely

caused by the balanced interaction of toluene and  $\text{NaNO}_3$  molecules adhered at the available surface active sites of  $\text{MoO}_3$ . Assuming that the toluene/ $\text{NaNO}_3$  reaction occurred between components located at neighboring active sites on surface of  $\text{MoO}_3$ , one expects that excess of toluene may lead to many active sites occupied by toluene with no nearby  $\text{NaNO}_3$ . In this case, the yield is reduced, as observed experimentally for low  $\text{MoO}_3$ /toluene ratios. The yield is also reduced, as expected, for very low  $\text{NaNO}_3$  concentrations.

The number of active sites is expected to increase as a function of the milling time or milling dose, explaining an observed greater mononitrotoluene yield for an increased milling dose. It is suggested that an increased amount of  $\text{MoO}_3$  should generally lead to a greater yield generating more active sites at which the reaction can occur.

It is less clear how the selectivity of toluene nitration was affected by the process parameters. A number of parameters, which were not carefully monitored, could have affected the selectivity, which justifies the need in an additional study. For example, the milling vial temperature, which is expected to vary as a function of the amount of toluene (serving also as a liquid process control agent and lubricant), the total solid load, BPR, and other parameters could have affected the selectivity substantially.

## 2.5 Conclusions

Feasibility of mechanochemical nitration of toluene is shown using  $\text{NaNO}_3$  as a reactant and  $\text{MoO}_3$  as a catalyst. This study is the first, to the authors' knowledge, to report nitration of toluene with molybdenum oxide - a safe to handle, relatively inert compound which has been reported to have weak Lewis acid properties. It does not catalyze the reaction between

NaNO<sub>3</sub> and toluene in a test tube, but under mechanical impact it was found to catalyze aromatic nitration, with the yields increasing with the amount of milling. Several other metal oxides were also explored as potential Lewis acids, including WO<sub>3</sub>, TiO<sub>2</sub>, Al<sub>2</sub>O<sub>3</sub> and ZrO<sub>2</sub> with negative results.

The yield exceeding 40% of mononitrotoluene has been attained, and a higher yield is expected to be possible with further optimization of the process parameters. An increase in yield is accompanied with a greater selectivity of preparation of mononitrotoluene, suggesting that a practical, solvent-free preparation of mononitrotoluene is possible. The reaction mechanism is likely affected by active sites generated on surface of MoO<sub>3</sub> during milling. Both toluene and NaNO<sub>3</sub> molecules are expected to adhere to the active sites and react most effectively when an optimized distribution of the reactants on the surface of the catalyst is achieved.

## CHAPTER 3<sup>2</sup>

### EFFECT OF PROCESS PARAMETERS ON MECHANOCHEMICAL NITRATION OF TOLUENE

#### 3.1 Introduction

Nitration of organic compounds is used in a wide variety of applications. The majority of energetic materials, for example, are organic compounds with the nitro group as the oxidizer[78]. Nitrated aromatics are also widely used as solvents, dyes [3], pharmaceuticals [5], and perfumes [79]. For energetic materials, nitrotoluene is of particular interest because it is the precursor in the synthesis of trinitrotoluene, a common explosive [7, 8]. In addition, nitrotoluene is used to synthesize nitrobenzaldehyde, toluidine, and chloronitrotoluenes – the intermediates in the production of dyes, resin modifiers, optical brighteners and suntan lotions [80]. The nitrating agent for these reactions has traditionally been fuming nitric acid combined with another strong acid, e.g., sulfuric acid, perchloric acid, selenic acid, hydrofluoric acid, boron trifluoride, or an ion-exchange resin with sulfonic acid groups. These acids are catalysts that help form the nitronium ion,  $\text{NO}_2^+$ . Sulfuric acid is most common in industrial nitration because it is both effective and relatively inexpensive.

The common nitration methods have a number of disadvantages, such as the production of large quantities of spent acid which must be regenerated because its neutralization and disposal on a large scale are environmentally and economically unsound [81]. Another issue is the generation of environmentally harmful waste during the purification of the products [15]. Additional disadvantages include the hazards of handling

---

<sup>2</sup> Article submitted to Journal of Materials Science, 2/18

the nitrating agents, and over-nitration [16]. The reactions involving strong acids are not selective and yield a mixture of isomers, some of which are less desirable than others. For example, toluene nitration produces a mixture of mononitrotoluene (MNT) isomers with 55-60% of ortho- or o-MNT, 35-40% of para- or p-MNT, and 3-4% of meta-, or m-MNT [80]. This leads to large quantities of unwanted product because the demand for p-MNT is greater than for the other isomers [17, 80]. To increase the ratio of p- to o- isomers, nitration is commonly done in the presence of phosphoric acid or aromatic sulfonic acids. While the p/o ratio increases from 0.6 to 1.1-1.5 [80], additional environmentally harmful reactants are used. Another challenge is the formation of oxidized byproducts. The addition of the nitro group to the aromatic ring of toluene strongly activates its methyl group towards oxidation, which is minimized in the industrial process by carrying it out at low temperatures [80]. In a batch process, for example, the acids are added at 25°C and the reaction is carried out at 35 – 40°C [80]. The total MNT yield in this reaction is 96% for a batch process, but most patents for continuous processes report yields of up to 50% [80].

Our previous study [82] established the feasibility of mechanochemical nitration of toluene using sodium nitrate as a source of nitronium ion, and molybdenum oxide as an environmentally benign catalyst. It was observed that the MNT production was strongly affected by the relative ratios of the starting components:  $C_7H_8$ ,  $NaNO_3$ , and  $MoO_3$ . While MNT was formed, the yield was relatively low and substantial amounts of undesired byproducts formed as well. The reaction mechanism had not been clarified. The objectives of the current work are, therefore, to improve the accuracy of product analysis, to identify experimentally the process parameters affecting yield and selectivity of MNT formation, and finally, to interpret the experimental parametric study of MNT production to elucidate the processes and reactions leading to the mechanochemical nitration of toluene.

## 3.2 Experimental

### 3.2.1 Sample Preparation

Following our previous work [82], toluene was nitrated by mechanical milling with sodium nitrate and molybdenum oxide. The bulk reaction is shown in Equation 2.1.

Materials used in the experiments were toluene (Startex, solvent grade), molybdenum oxide (Alfa-Aesar, 99.95 %), and sodium nitrate (Alfa Aesar, 99%). Several milling runs were carried out with a fraction of  $\text{MoO}_3$  substituted with silica. Two types of silica were used: fumed silica (Alfa Aesar, 99.8%) and quartz glass obtained by crushing quartz glass cylinders with a hammer and pre-milling it in a shaker mill for 5 minutes. The reactants were milled in a Retsch PM 400MA planetary mill using hardened steel vials and hardened steel balls or glass beads as milling media. The milling media varied as listed in Table 3.1.

**Table 3.1** Milling Media

| Media                | Diameter                          |
|----------------------|-----------------------------------|
| Hardened Steel Balls | 1/2" = 12.7 mm                    |
|                      | 3/8" = 9.525 mm                   |
|                      | 1/4" = 6.35 mm                    |
|                      | 1/8" = 3.175 mm                   |
| Glass Beads          | 0.4-0.6 mm (average 0.5 mm)       |
|                      | 0.088-0.149 mm (average 0.125 mm) |

The total mass of the solids in each vial was kept constant at 43.3 g, including 1.67 g of sodium nitrate. The volume of toluene was 0.5 ml for most runs, although several samples were prepared with 2 ml toluene. The mass of the milling media was 130 g for all runs, thus the ball to powder mass ratio (BPR) stayed constant at 3. Milling times varied from 0.5 to 4 hrs. All samples were milled at 400 RPM.

In all experiments, the vials were cooled using an air conditioner unit, built into the planetary mill and set at 15.6 °C (60 F). The milling temperature was adjusted further by using custom-made cooling fins (see [83] for details) added to the vials and by employing an intermittent milling protocol. The surface temperatures of the milling vial lids were measured during several runs using previously calibrated thermistors attached to the lids. The readings were taken at half hour intervals throughout the runs. Details of the three temperature control regimes and respective temperatures are listed in Table 3.2. The differences in the vial temperatures associated with the different milling protocols are around 20-25 °C. It is apparent that the milling media had no effect on the vial temperature except for the case of milling with 1/2" steel balls, in which the total number of balls was considerably smaller than in other cases. In the latter case, the temperature was reduced noticeably compared to all other milling media. Additional measurements (omitted from Table 3.2 for brevity) showed that replacing a fraction of MoO<sub>3</sub> with silica had no effect on the vial temperature for any of the temperature control regimes.



**Table 3.2** Temperature Control Regimes of Planetary Mill Experiments

| Milling balls (media) |                        | Temperature, °C for different milling protocols |   |  |
|-----------------------|------------------------|---|---|--|
| Material              | Diameter,<br>inch (mm) | Intermittent<br>milling, fins<br>"Low"          | Continuous<br>milling, fins<br>"Intermediate" | Continuous<br>milling, no fins<br>"High" |
| Glass                 | 0.125 mm               |   | 47.3±3.3                                      |  |
| Glass                 | 0.50 mm                |   | 44.8±0.2                                      | 63.5±3.2                                 |
| Hardened Steel        | 1/8 (3.175)            | 19.0±1.0  | 47.8±2.9                                      | 68.2±5.7                                 |
| Hardened Steel        | 1/4 (6.35)             | 22.3±5.5  | 47.0±4.4                                      | 69.6±2.7                                 |
| Hardened Steel        | 3/8 (9.525)            |   | 47.3±3.7                                      |  |
| Hardened Steel        | 1/2 (12.7)             |   | 34.2±0.3                                      | 42.5±11.7                                |

Based on literature reports of aromatic nitration with fuming nitric acid using MoO<sub>3</sub> on silica support as the catalyst [21], we investigated the possibility of toluene nitration by substituting part of the MoO<sub>3</sub> catalyst with silica. Several 2-hr milling runs were carried out in the planetary mill with varying fractions of MoO<sub>3</sub> replaced with silica. 1/4" hardened steel balls were used as milling media in all of these runs. All three temperature control regimes listed in Table 3.2 were used with fumed silica; only the intermediate protocol was used with quartz glass.

### 3.2.2 Sample Recovery

Reaction products were extracted with ethyl acetate (Alfa Aesar, 99.5 %). Before extraction, the milling vials were allowed to cool for 20 minutes by being left in the mill with the air conditioner running. Each milling vial was then opened and 150 ml of ethyl

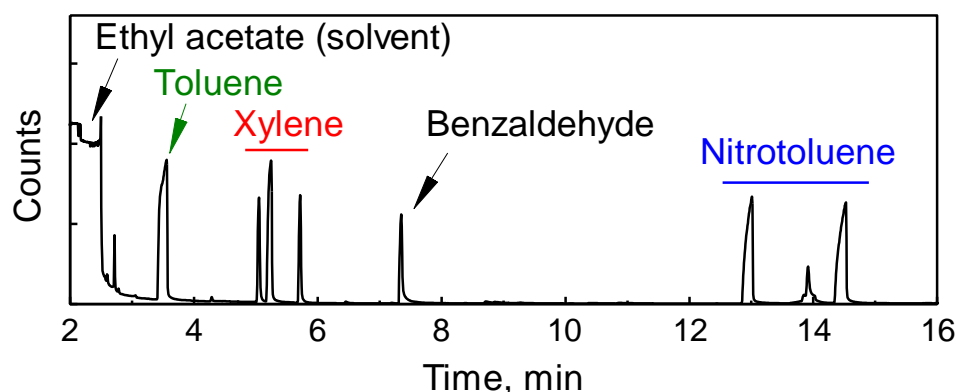
acetate were added to the vial. The vial was closed and placed back in the mill, where it was spun at 300 RPM for 5 min, with balls remaining in the vial, in order to agitate the suspension. This suspension was then stored for further analysis. In two experiments, samples were extracted using a water-cooled 500 ml Soxhlet extractor. The solvent was added into the milling vial and agitated at 300 RPM for 1 minute. The resulting suspension was removed and added into the thimble of the extractor until it was filled. The thimble was then placed in a beaker and kept there until the liquid fraction collected in the beaker. The procedure was repeated until the entire sample was filtered. Then the thimble was placed into the extractor and the solution recovered from the beaker was placed into the extractor flask and boiled for 24 hours with the aid of boiling stones.

### 3.2.3 Sample Analysis

Each suspension sample was stirred and the solid fraction was separated by centrifuging for 5 minutes in a LW Scientific Ultra-8F centrifuge. The liquid fraction was analyzed in an HP 6890 gas chromatograph (GC, heating profile: 40 °C to 250 °C at 5 K/min; split ratio: 10) coupled with HP G2350A mass spectrometer (MS). Product species were identified using the NIST Mass Spectral Library (NIST 08). Different data processing methods were used to evaluate concentrations of the products using the GC-MS output. In preliminary experiments, as in Ref. [82], the relative yield of MNT,  $Y_{MNT,rel}$ , was estimated as

$$Y_{MNT,rel} = \frac{\sum P_{MNT}}{P_{Tol} + \sum P_{products}} \quad (3.1)$$

where  $P$  indicates the integrated GC peaks, and the subscripts refer to MNT, toluene, and all identifiable products, respectively. Similarly, the relative yield of any species can be estimated for all products by using their respective peak areas in the numerator. Using Equation (3.1) to calculate the product yield introduces several potential errors. In addition to measurement uncertainties, any underestimation of the amounts of toluene and reaction products, whether due to losses or due to the presence of additional products undetected by GC-MS, leads to systematic overestimation of the MNT yield. In order to mitigate some of these uncertainties, the yield was determined relative to the amount of toluene introduced at the beginning of milling. This required calibration of the GC-MS measurements. To achieve that, a known amount of xylene (Sunnyside, solvent grade) was added to the ethyl acetate solution as an internal standard for each subsequent measurement. Figure 3.1 shows a sample GC-MS plot featuring xylene and MNT peaks.



**Figure 3.1** Sample GC-MS trace of a processed sample with xylene added as an internal standard.

In addition to MNT peaks, benzaldehyde (labeled in Figure 3.1) as well as two dimers: 2-methylphenyl-phenylmethanone and 4-methylphenyl-phenylmethanone (occurring at longer times than included in the figure) were consistently observed as formed

byproducts. These species were accounted for when assessing the total recovery of the products of mechanochemical reaction from the milling vials, as discussed below.

The GC peak areas for MNT and toluene were calibrated using reference solutions of toluene, p-MNT (Sigma-Aldrich, 99%), and xylene in ethyl acetate. Actual concentrations could then be determined from the recorded calibration curves and peak ratios of MNT and toluene respectively, to xylene. The absolute yield of MNT,  $Y_{MNT}$ , was calculated as

$$Y_{MNT} = \frac{f_{MNT} \left( \sum P_{MNT} / \sum P_{xyl} \right) \cdot C_{xyl}}{C_{tol,0}} \quad (3.2)$$

where  $f_{MNT}$  indicates the calibration curve discussed above,  $P_{xyl}$ , and  $C_{xyl}$  are the peak areas and introduced concentrations of xylene, respectively.  $C_{tol,0}$  is the initial toluene concentration at the beginning of milling.

The yield determined using Equation (3.2) may be lower than the true yield, because of incomplete recovery of products. Product recovery,  $R$ , was therefore assessed as:

$$R = \frac{\sum_{products} C_i}{C_{tol,0}} \quad (3.3)$$

where the sum in the numerator contains all toluene-derived species determined by GC-MS, including toluene itself. In this estimate, product species concentrations that were not explicitly calibrated, were estimated by setting their respective calibration function,

$f_i(\sum P_i / \sum P_{xy}) = 1$ . This leads to unspecified systematic errors, which can only be corrected if a specific calibration is performed for each species formed. However, the purpose of this analysis is the relative comparison between different runs; therefore, a repeatable systematic error is acceptable.

### **3.2.4 Surface Area Measurements**

Surface area of the solid fraction of several samples was determined using Brunauer–Emmett–Teller (BET) nitrogen adsorption method. After extracting the organic phase, the solid (inorganic phase) was dried and degassed at 350°C for 4.5 hours. After degassing, the surface area of the samples was measured using nitrogen adsorption BET (Quantochrome Instruments Autosorb IQ ASIQM000000-6, 11 point adsorption measurement).

## **3.3 Results**

### **3.3.1 Preliminary Experiments**

In the preliminary experiments, milling times varied from 1 to 4 hours; different milling media were used; and the relative MNT yield was obtained from Equation (3.1). Significant relative yields of MNT, in the range of 10% – 90% were observed for all milling conditions, including the experiments with glass beads as the milling media. Results with different milling media showed the lowest yields when 12-mm steel balls were used. The yields were also relatively low for glass beads. The highest yields were obtained for the milling times of 1-2 hours when 3 – 10-mm diameter hardened steel balls served as the milling media. It was also observed that the recovery of the product using Soxhlet extractor was

not more effective than using the solution agitated in the mill; consequently, the latter approach was employed in all experiments discussed below.

All systematic experiments are summarized in Table 3.3. The highest observed mononitrotoluene yield exceeded 65 %, and the ratio of para to ortho isomers was consistently above 1.

Observed trends are discussed in detail below.

**Table 3.3** Summary of Systematic Experiment Data (Continued)

| Milling Media Size, in | % SiO <sub>2</sub> | Toluene Initial Volume mL | Milling Time, hrs | Temp. Regime | Est. temp. °C | Surface Area, m <sup>2</sup> /g | MNT Yield,% | p/o Ratio |
|------------------------|--------------------|---------------------------|-------------------|--------------|---------------|---------------------------------|-------------|-----------|
| 1/2                    | 0                  | 0.5                       | 0.5               | I            | 31.6          |                                 | 11.0        | 1.02      |
| 1/2                    | 0                  | 0.5                       | 1                 | I            | 31.6          |                                 | 21.1        | 1.07      |
| 1/2                    | 0                  | 0.5                       | 2                 | H            | 50.6          | 10.8                            | 23.3        | 0.64      |
| 3/8                    | 0                  | 0.5                       | 0.5               | I            | 47.3          |                                 | 32.2        | 1.16      |
| 3/8                    | 0                  | 0.5                       | 1                 | I            | 47.3          |                                 | 54.8        | 1.15      |
| 1/4                    | 0                  | 0.5                       | 0.5               | I            | 49.8          |                                 | 45.5        | 1.21      |
| 1/4                    | 0                  | 0.5                       | 1                 | I            | 49.8          |                                 | 67.3        | 1.25      |
| 1/4                    | 10                 | 0.5                       | 2                 | L            | 33.4          |                                 | 33.4        | 1.36      |
| 1/4                    | 10                 | 0.5                       | 2                 | I            | 49.8          |                                 | 31.8        | 1.40      |
| 1/4                    | 10**               | 0.5                       | 2                 | I            | 49.8          |                                 | 23.0        | 1.41      |
| 1/4                    | 10                 | 0.5                       | 2                 | H            | 68.8          |                                 | 44.4±0      | 1.13±.12  |
| 1/4                    | 20                 | 2                         | 2                 | I            | 49.8          |                                 | 9.7         | 1.14      |
| 1/4                    | 20                 | 0.5                       | 2                 | H            | 68.8          |                                 | 44.2        | 1.12      |
| 1/4                    | 30                 | 0.5                       | 2                 | L            | 33.4          | 35.8                            | 49.6±7.2    | 1.34±.06  |
| 1/4                    | 30**               | 0.5                       | 2                 | I            | 49.8          |                                 | 40.3        | 1.30      |
| 1/4                    | 30                 | 0.5                       | 2                 | I            | 49.8          | 45.8                            | 55.4±7.8    | 1.26±.01  |
| 1/4                    | 30                 | 0.5                       | 2                 | H            | 68.8          |                                 | 61.7        | 1.37      |
| 1/4                    | 40                 | 0.5                       | 2                 | H            | 68.8          |                                 | 55.4        | 1.13      |
| 1/4                    | 50                 | 0.5                       | 2                 | L            | 33.4          |                                 | 36.4        | 1.25      |
| 1/4                    | 50                 | 0.5                       | 2                 | I            | 49.8          |                                 | 42.9±17.4   | 1.39±.02  |
| 1/4                    | 50**               | 0.5                       | 2                 | I            | 49.8          |                                 | 12.1        | 1.00      |
| 1/4                    | 50                 | 2                         | 2                 | I            | 49.8          |                                 | 10.6        | 1.14      |
| 1/4                    | 50**               | 2                         | 2                 | I            | 49.8          |                                 | 7.5         | 1.13      |
| 1/4                    | 50                 | 0.5                       | 2                 | H            | 68.8          |                                 | 26.7±1.6    | 1.19±.13  |
| 1/4                    | 70                 | 0.5                       | 2                 | I            | 49.8          |                                 | 4.5         | 1.47      |
| 1/4                    | 70**               | 0.5                       | 2                 | I            | 49.8          |                                 | 8.3         | 1.01      |
| 1/4                    | 90                 | 0.5                       | 2                 | I            | 49.8          |                                 | 0.3         |           |

**Table 3.3** (Continued) Summary of Systematic Experimental Data

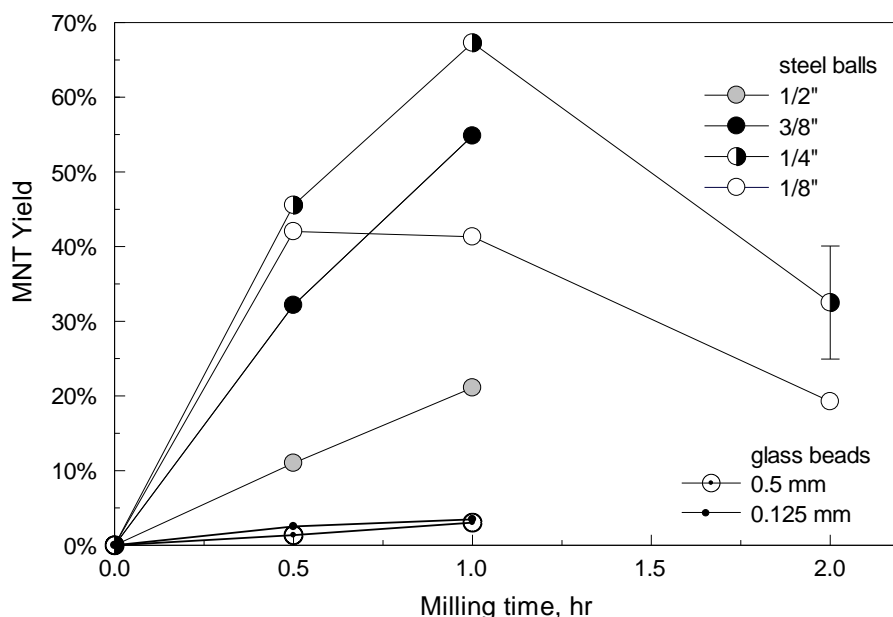
| Milling Media Size, in | % SiO <sub>2</sub> | Toluene Initial Volume mL | Milling Time, hrs | Temp. Regime | Est. temp. °C | Surface Area, m <sup>2</sup> /g | MNT Yield,% | p/o Ratio |
|------------------------|--------------------|---------------------------|-------------------|--------------|---------------|---------------------------------|-------------|-----------|
| 1/4                    | 0                  | 0.5                       | 2                 | L            | 33.4          | 14.5                            | 33.6±11.6   | 1.34±.01  |
| 1/4                    | 0                  | 0.5                       | 2                 | I            | 49.8          | 18.5                            | 32.5±7.6    | 1.36±.08  |
| 1/4                    | 0                  | 0.5                       | 2                 | H            | 68.8          | 15.3                            | 32.3±1.4    | 1.25±.01  |
| 3/16                   | 0                  | 0.5                       | 0.5               | I            | 48.5          |                                 | 42.0        | 1.19      |
| 3/16                   | 0                  | 0.5                       | 1                 | I            | 48.5          |                                 | 41.3        | 1.28      |
| 3/16                   | 30                 | 0.5                       | 2                 | I            | 48.5          | 44.8                            | 48.5        | 1.26      |
| 3/16                   | 30                 | 0.5                       | 2                 | L            | 32.1          | 43.3                            | 36.7        | 1.20      |
| 3/16                   | 0                  | 0.5                       | 2                 | L            | 32.1          | 11.5                            | 12.3        | 1.41      |
| 3/16                   | 0                  | 0.5                       | 2                 | I            | 48.5          | 13.1                            | 19.2        | 1.43      |
| 0.5*                   | 0                  | 0.5                       | 0.5               | I            | 44.6          |                                 | 1.4         | 1.24      |
| 0.5*                   | 0                  | 0.5                       | 1                 | I            | 44.6          |                                 | 3.0         | 1.23      |
| 0.5*                   | 0                  | 0.5                       | 2                 | H            | 63.6          | 15.4                            | 20.6        | 1.17      |
| 0.125*                 | 0                  | 0.5                       | 0.5               | I            | 47.3          |                                 | 2.5         | 1.11      |
| 0.125*                 | 0                  | 0.5                       | 1                 | I            | 47.3          |                                 | 3.5         | 1.30      |

\* glass beads, mm units

\*\* quartz glass instead of fumed silica

### 3.3.2 Effect Of Milling Time And Media

Absolute MNT yield calculated using Equation 3.2 is shown in Figure 3.2 for a set of experiments with varied milling times and milling media. The milling protocol employing continuous milling with cooling fins (leading to intermediate vial temperatures, see Table 3.2) was used in all experiments shown. No silica was used. As seen in the figure, the highest MNT yields occur close to 1 hour for runs using 1/4" steel balls as the milling media. Results shown in Figure 3.2 also suggest that the peak yield may occur at shorter times for 1/8" steel balls, and possibly at longer times for larger steel balls, although additional measurements would be needed to confirm this. For any of the glass beads used, the yield is substantially lower than for any runs using steel balls for the set of measurements shown in Figure 3.2.

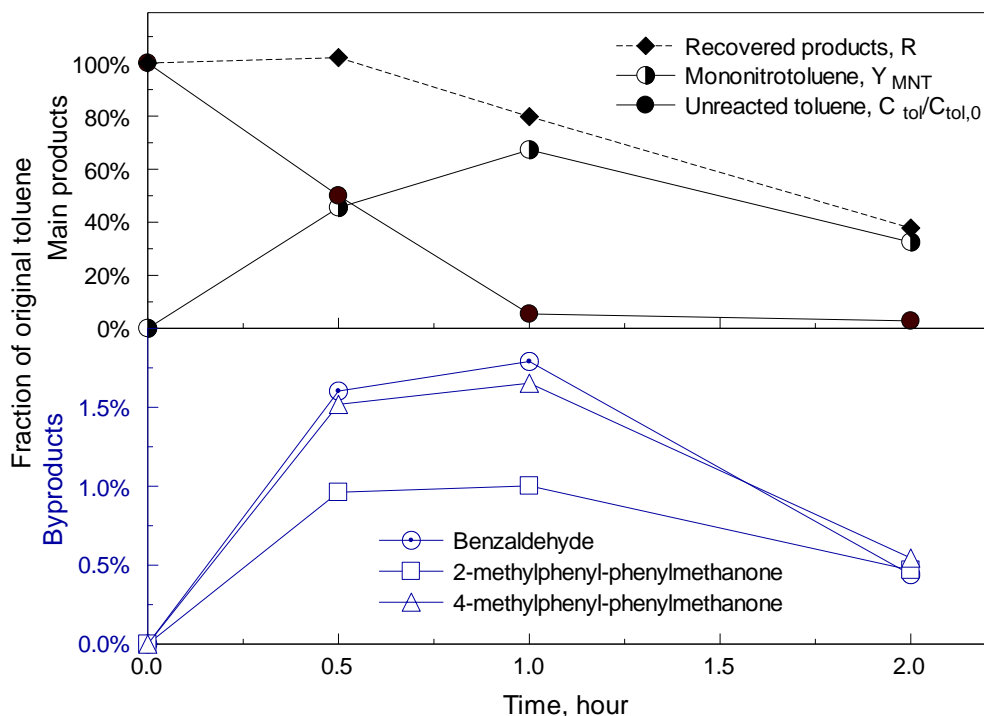


**Figure 3.2** Absolute MNT yield for different milling times and milling media. The intermediate temperature regime was used.

To understand the reasons for the reduction in the MNT yield at longer milling times, clearly observed for the cases of 1/8" and 1/4" steel balls, consider data presented in Figure 3.3. Results for 1/4" steel balls, for which the highest MNT yield was observed, are examined closer. The recovery and MNT yield for that case are compared to the fraction of toluene left in the vial and the fractions of the consistently observed byproducts. All the concentrations were determined by comparing the measured GC-MS peak areas of respective species to that of xylene, while accounting for the actual xylene concentration; then the fraction of each compound was assessed based on the starting amount of toluene, similar to Equation 3.3. As noted earlier, because no xylene-based calibration was made for the byproducts, the concentrations may include a systematic error. However, the main purpose of introducing such concentrations here is to observe their relative changes as functions of milling time. Therefore, a systematic error is acceptable, as long as all the data is processed consistently. Results in Figure 3.3 show that most of toluene was consumed by the end of 1-hr milling, when the peak MNT yield was observed. The highest MNT



yield occurs at the same time as the peak concentrations of all tracked byproducts. At longer milling times, MNT concentration as well as the byproduct concentrations decrease, while the toluene concentration remains negligible. The reduced recovery at longer milling times could represent either additional reactions in the milling vial, with products that are not detectable by GC-MS, or physical losses during milling or the extraction procedure.

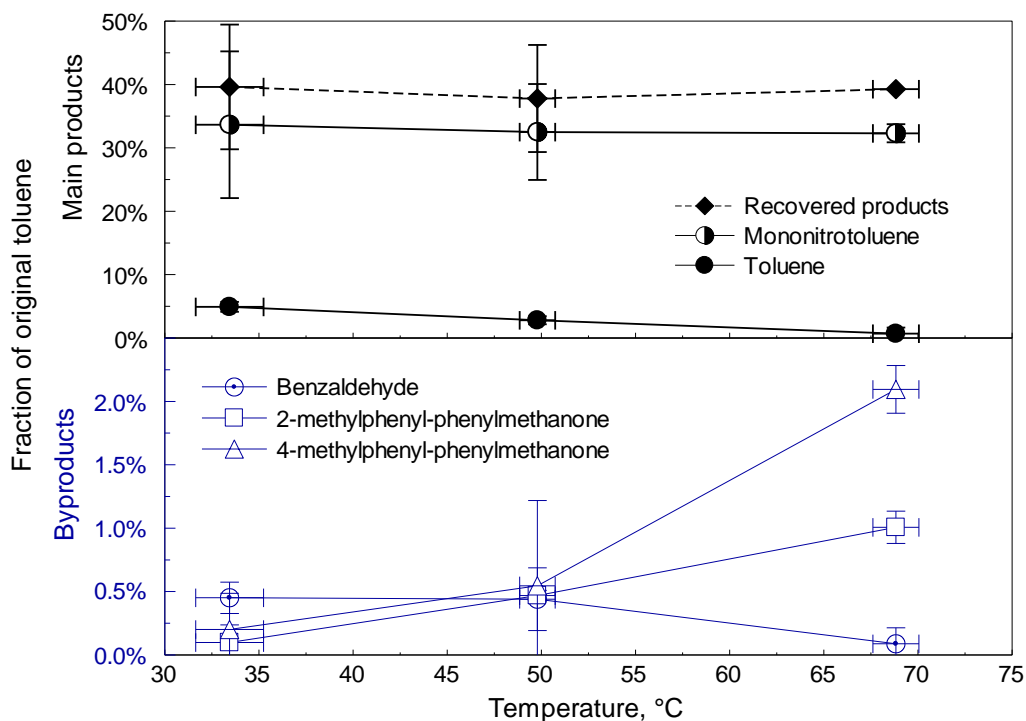


**Figure 3.3** Comparison of the total product recovery, absolute MNT yield, and depletion of toluene along with yields of significant byproducts as functions of milling time. 1/4" steel milling balls have been used with the intermediate temperature regime.

### 3.3.3 Effect of Temperature

Figure 3.4 shows the MNT yield as function of effective milling temperature for 1/4" steel balls, after 2 hours of milling. The error bars show standard deviations from repeat experiments. The overall yield is effectively constant with temperature. The toluene recovery is inversely proportional to the milling temperature, although most of toluene is consumed at all temperatures, consistent with the trends seen in Figure 3.3. However, increased losses at higher temperatures cannot be ruled out. On the other hand, the

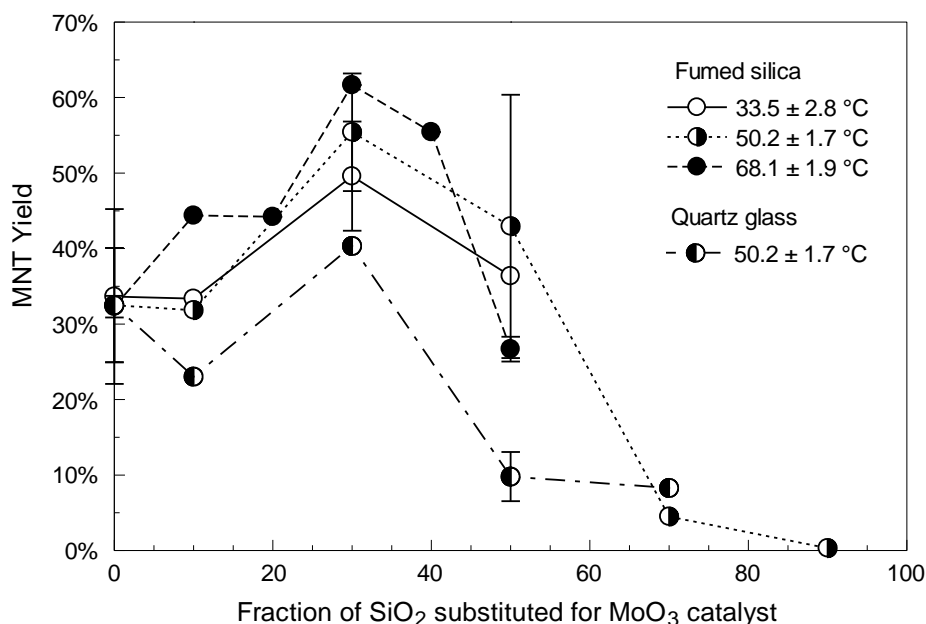
formation of different byproducts follows different trends. Benzaldehyde is more abundant at low temperatures, while its yield at the higher temperature is reduced. Conversely, the yield of both dimers consistently increases with temperature; a trend opposite to that observed for the total product recovery. Inspecting data in Table 3.3 shows that the p/o ratio for the MNT isomers varies in the range of ca. 1.25-1.35 with a slightly greater p/o ratio at lower milling temperatures.



**Figure 3.4** Comparison of the total product recovery, absolute MNT yield, and depletion of toluene along with the yield of significant byproducts, as functions of milling temperature. 1/4" steel balls are used. The milling time is 2 hours.

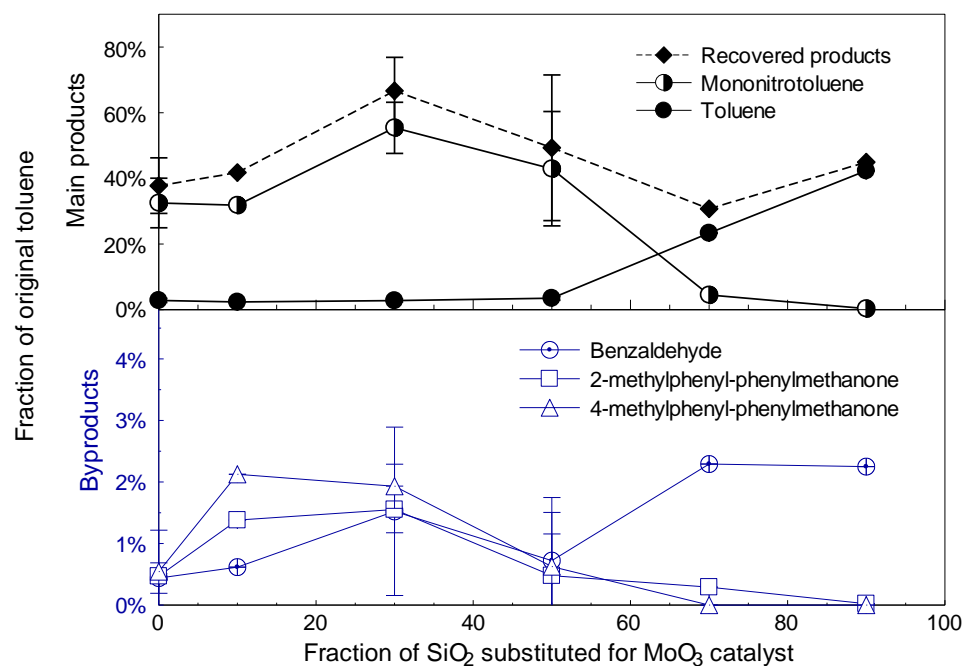
### 3.3.4 Milling with MoO<sub>3</sub> and Silica

The absolute MNT yield calculated using Equation (3.3) is shown in Figure 3.5 for multiple experiments performed at a fixed milling time of 2 hours, in which a fraction of MoO<sub>3</sub> was replaced with silica. Different milling protocols resulting in different temperatures were used; both fumed silica and quartz glass were used in different runs. The results show clearly that the MNT yield is highest when about 30 wt % of MoO<sub>3</sub> are replaced with silica. This effect is the same for both fumed silica and quartz glass, although quartz glass gives systematically lower yields than fumed silica. Consequently, the experiments with quartz glass were performed using only one milling protocol. At different temperatures, the maximum yield is observed at about the same fraction of MoO<sub>3</sub> replaced with fumed silica. The lack of a pronounced effect of milling temperature on yield, observed in Figure 3.4 is generally consistent with the results shown in Figure 3.5. For both fumed silica and quartz glass, an increase in the silica content well above 30% causes a substantial reduction in the yield. Data in Table 3.3 show no correlation between p/o ratio of the produced MNT isomers and fraction of SiO<sub>2</sub> substituting MoO<sub>3</sub>.



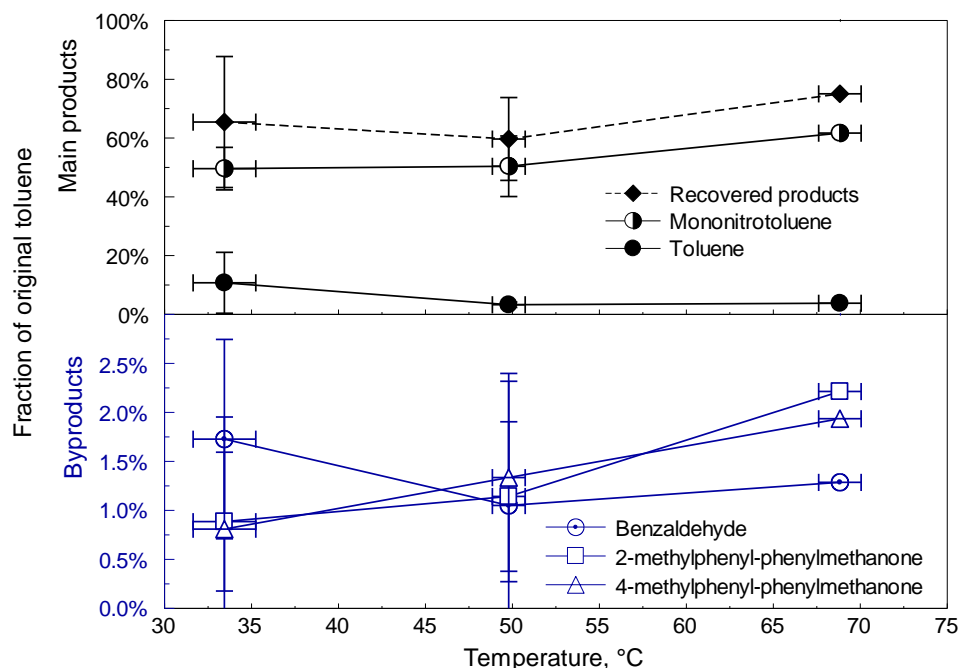
**Figure 3.5** Absolute MNT yield vs. fraction of silica replacing MoO<sub>3</sub> for 2-hr runs using 1/4" steel balls as milling media.

In Figure 3.6, the MNT yield is plotted along with the recovery, yields of byproducts, and amount of toluene left for different fractions of silica replacing MoO<sub>3</sub> for the set of experiments with 1/4" steel balls. Initially, both MNT yield and the recovery increase with greater amounts of silica used. Above about 30 % silica, a clear trend of increased toluene concentration (along with the reduced MNT yield) is observed, indicative of an overall lower reaction rate caused by the dilution of the MoO<sub>3</sub> catalyst. The trends observed for byproducts are somewhat different: benzaldehyde forms preferentially at greater silica amounts. Both dimers form with a pattern closely following the formation of MNT. It is interesting that despite greater concentrations of unreacted toluene at high silica amounts, the recovery is relatively low.



**Figure 3.6** Comparison of the total product recovery, absolute MNT yield, and depletion of toluene along with the yield of significant byproducts as functions of the added silica. 1/4" steel milling balls are used with the intermediate temperature milling protocol. Milling time is 2 hours.

Figure 3.7 shows product yields and recovery rates vs. temperature for the experiments with 30 % of the MoO<sub>3</sub> catalyst replaced by fumed silica. A weak positive trend in the MNT yield is observed. The dimeric byproducts also increase with increasing temperature, similarly to the results in Figure 3.4 when no silica was added. From Table 3.3 it can be noted that the p/o ratio increases slightly at reduced milling temperatures, consistent with the observation for experiments performed at different temperatures but without silica.



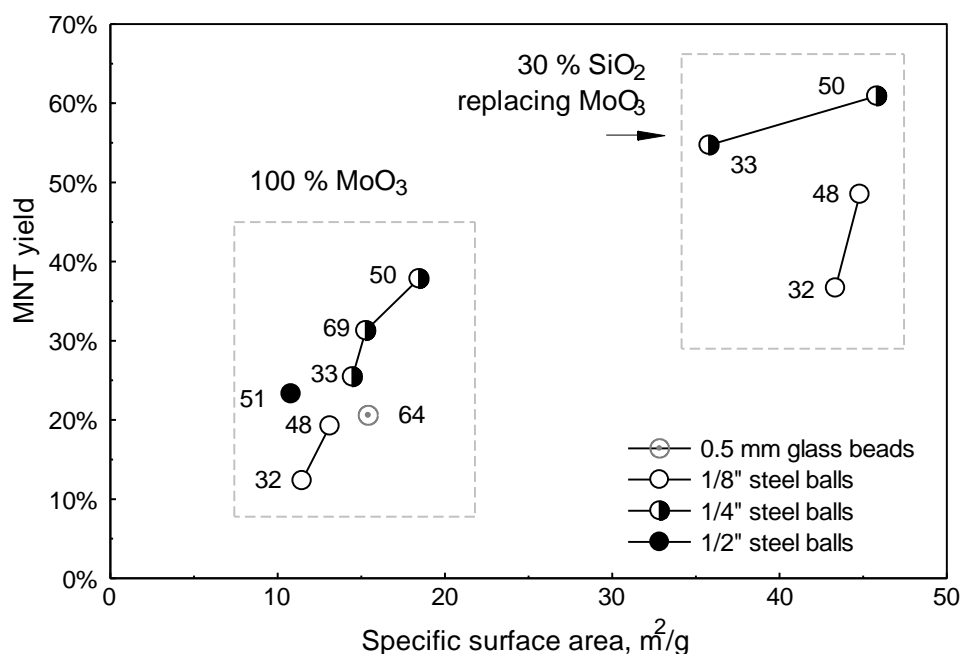
**Figure 3.7** Product recovery, absolute MNT yield, and toluene consumption as a function of milling temperature with yield of significant byproducts when 30 % of the  $\text{MoO}_3$  catalyst is replaced with fumed silica. 1/4" steel balls are used with the milling time of 2 hours.

### 3.3.5 Surface Area Measurements

Surface areas of the inorganic fraction of the milled samples were measured for several 2-hour planetary mill runs with varying milling media, with and without silica. For the samples without silica, specific surface areas ranged from  $10.4 \text{ m}^2/\text{g}$  to  $18.5 \text{ m}^2/\text{g}$ , whereas for the samples milled with 30% silica specific surface areas ranged from 35 to  $45 \text{ m}^2/\text{g}$ . The surface area of unmilled fumed silica was determined to be  $484 \text{ m}^2/\text{g}$ ; thus the surface area of the milled samples was significantly less than the sum of the surface areas of the separate sample components. This indicates that the silica was incorporated within the molybdenum oxide to form composite catalyst particles.

Figure 3.8 shows the MNT yields determined for a set of 2-hour experiments with corresponding surface area measurements. This plot combines results obtained with different milling media, including samples prepared with and without 30 %  $\text{SiO}_2$

substituted for the  $\text{MoO}_3$  catalyst. In addition, effective milling temperatures are indicated at each data point. There appears to be an overall positive correlation between specific surface area and MNT yield. As shown in Figures 3.4 and 3.5, MNT yield may also be positively correlated with the milling temperature, although the effect is weak. No correlation between specific surface area and p/o ratio of the produced MNT isomers was detected from data in Table 3.3.



**Figure 3.8** Absolute MNT yield as a function of the surface area of the milled solids. Milling time is 2 hours. Data point labels show effective milling temperatures in  $^{\circ}\text{C}$ .

### 3.4 Discussion

In the previous experiments, primarily using a shaker mill [82], it was observed that the reaction yield increased substantially with an increase of solid (catalyst) to liquid (toluene) ratio. The present results, using a planetary mill enabled us to increase considerably the solid to liquid ratio and to achieve respectively higher yields.

Variations in the yield of MNT as a function of different process parameters observed in this study suggest that the mechanochemical reaction of nitration of toluene is relatively complex. As with other mechanochemical reactions, one can initially assume that the reaction rate is proportional to the collision frequency of the milling media; it is further of interest to consider whether the energy dissipated in such collisions is affecting the reaction effectiveness or rate. Finally, it is of interest to consider how the temperature and catalyst properties affect the reaction.

To assess the effect of collision frequency on the reaction rate, consider the results with different milling media sizes shown in Figure 3.2. A possible shift in the maximum yield of MNT to greater milling times for greater ball sizes supports the idea of reaction rate scaling with collision frequency, clearly increasing for smaller balls. At the same time, a reduced absolute maximum yield of MNT for 1/8" steel balls compared to that for 1/4" steel balls suggests that the energy dissipated in collisions affects the reaction effectiveness. The latter conclusion is also consistent with the results of experiments with glass beads. The number of collisions in those experiments was increased greatly; yet, the MNT yield was quite low, suggesting that the reaction does not occur effectively when the collision energies are low.

It is tempting to assign significance to the optimized milling conditions, including milling time of 1 hr (Figure 3.2) and added 30% of fumed silica (Figure 3.5) for the yield of MNT observed experimentally. However, the measurements showing the effects of time and silica addition represent both the MNT formation reaction and secondary product formation, or physical losses, as emphasized by the reduced recovery rate seen in Figures 3.3 and 3.6. For the effect of time, in particular (Figure 3.3), yield of all byproducts and recovery essentially follow each other after the maximum yield is achieved. Importantly,



the toluene consumption continues to increase for longer milling times despite the reduced yield of all products. The product recovery reduced at greater milling times, might be caused by greater adsorption of products to  $\text{MoO}_3$  particles. The latter could be contributed to modification of  $\text{MoO}_3$  surface by the greater number of collisions. Separating the effects of product recovery and optimized yield of MNT needs to be addressed in future work. For example, using solvents other than ethyl acetate employed in the present study may be considered. Alternatively, the reduced recovery rate could be related to secondary products that are not captured by the current extraction technique, such as gases caused by over-oxidation of any of the organic materials.

In case of added silica, the recovery improves with the silica fraction increasing above 70% (Figure 3.6), while the MNT yield decays, clearly suggesting that it is  $\text{MoO}_3$  and not  $\text{SiO}_2$  that catalyzes the reaction. Additional experiments at shorter milling times as the most readily controlled experimental parameter may be needed to establish quantitative trends describing the MNT formation alone.

Although the MNT yield and product recovery correlate with each other for the experiments performed at different temperatures (Figure 3.4), the yields of both dimers, important reaction byproducts, follow a different trend. An increase in the production of dimers at elevated temperatures suggests a change in the reaction mechanism or an accelerated decomposition of the produced MNT, when the process temperatures are higher. These observations suggest that describing the present mechanochemical reaction theoretically would not be successful if only one global reaction, e. g. reaction 2.1 is assumed. Additional reactions need to be included, which would account for direct formation of byproducts and, possibly, for decomposition of the generated MNT. Such additional reactions are also necessary to interpret the results shown in Figure 3.6: at 90 %

of silica added, effectively no MNT was produced (less than 1 %, Figures 3.5, 3.6), while concentration of benzaldehyde was rather significant (more than 2 %). Benzaldehyde, which is a typical product of oxidation of toluene, is formed by direct oxidation of toluene in the presence of  $\text{NaNO}_3$  and  $\text{MoO}_3$ .

To consider the effect of added silica on the MNT yield (Figure 3.5), which was maximized when 30% of silica were added, one may need to account for the combined effect of the remaining catalyst ( $\text{MoO}_3$ ) and an increased surface area of the solid caused by the added silica. The increased surface area is expected to lead to a greater number of mechanically activated reaction events, or greater overall reaction rate. The presence of  $\text{MoO}_3$  should account for an effective formation of MNT once the reaction is mechanically activated. It is unlikely that adding relatively small amounts of silica affected significantly the rate of reaction because the peak of MNT yield was observed for the same fraction of silica replacing  $\text{MoO}_3$  when different types of silica were used (Figure 3.5), which were expected to produce different surface areas available for the reaction. The yield peak at about 30% of silica is likely associated with the specific  $\text{MoO}_3/\text{SiO}_2$  ratio, which could affect catalytic activity of  $\text{MoO}_3$ , e.g., by altering a balance between Lewis and Brønsted acid sites in  $\text{MoO}_3$  [84]. It was also reported that silica can interact with  $\text{MoO}_3$  and improve its catalytic activity by forming polymolybdates [21]. Still, another possibility is that the added silica helps generating defects, serving as active sites on  $\text{MoO}_3$ . The effect of catalyst and its support require further investigation, which can be warranted if the mechanochemical nitration of toluene is to be developed for practical applications.

The relationship between the observed MNT yield, possible reaction mechanism, and the surface area of the solids should also be briefly discussed. Table 3.4 shows selected surface area measurements for 1/8" and 1/4" steel balls with and without 30 % silica, milled

in the intermediate temperature regime at effectively  $50.2 \pm 1.7$  °C. Taking the size of the toluene molecule as about 6 Å, derived from its molar volume, the corresponding coverage of the available surface with a toluene monolayer was estimated, and is shown in Table 3.4. A similar estimate is made and shown for MNT as well. The available toluene, if spread uniformly across all solid surface, may form 1-2 monolayers in the cases without silica. It may only form a discontinuous monolayer in the case with silica. In both cases, the estimates suggest that the reaction occurs heterogeneously at the surface in a very thin liquid layer, with properties distinctly different from that of a bulk liquid. The data in Table 3.4 may also suggest that without silica, the available catalyst surface may be rate limiting, while the catalyst surface could be more effectively used with the high-surface area fumed silica added. Note that the formed MNT can only cover a fraction of the available surface and thus is unlikely to result in a substantial reduction in the available catalyst surface. Clearly, such assessments are approximate and combine the toluene present in the milling vial at the beginning of the run with the solid surface measured after the experiment. As the milling run progresses, the amount of toluene decreases. In runs without silica, the solid surface is expected to increase, at least initially; conversely, the surface is decreasing with time in runs with silica present. Despite the general decrease in the surface area in the latter case, the surface of composite  $\text{MoO}_3/\text{SiO}_2$  particles acting as the catalyst, must be increasing.

**Table 3.4** Selected Surface Area Measurements and Surface Coverage Estimates

| Sample ID | Ball diameter | silica fraction | SA, m <sup>2</sup> /g | surface coverage       |           | surface coverage   |
|-----------|---------------|-----------------|-----------------------|------------------------|-----------|--------------------|
|           |               |                 |                       | with toluene monolayer | MNT yield | with MNT monolayer |
| 610A      | 1/8"          | 0 %             | 13.1                  | 147 %                  | 19.3%     | 28 %               |
| 610B      | 1/4"          | 0 %             | 18.4                  | 104 %                  | 37.9%     | 39 %               |
| 610C      | 1/8"          | 30 %            | 44.8                  | 43 %                   | 48.5%     | 21 %               |
| 610D      | 1/4"          | 30 %            | 45.8                  | 42 %                   | 60.9%     | 25 %               |

### 3.5 Conclusions

It is observed that high, practically significant yields of MNT, are attainable by mechanochemical reaction of toluene and sodium nitrate with molybdenum oxide as a catalyst, and without any added solvents. The reaction occurs with a high MNT yield when the ratio of liquid to solid is low, so that toluene is effectively spread in a monolayer on the surface of the catalyst. The rate of the mechanochemical nitration increases with the number of collisions; the reaction efficiency is also strongly affected by the energy dissipated in the collisions. Adding silica to the catalyst MoO<sub>3</sub> increases efficiency of the mechanochemical nitration of toluene as long as a sufficient amount of the catalyst remains available. The results suggest that introducing one global reaction may be inadequate for modeling mechanochemical nitration of toluene. Yields, which were optimized at a specific milling time and with specific silica content, will need to be described using additional reactions. Additional reactions are also necessary to describe the observed formation of

byproducts observed in the experiments, which were also affected by the milling temperature. At low concentrations of catalyst, direct oxidation of toluene by sodium nitrate can generate benzaldehyde, one of the main byproducts. No evidence is found of formation of dimers, 2-methylphenyl-phenylmethanone and 4-methylphenyl-phenylmethanone, other significant byproducts, by reactions directly involving toluene. Further work is needed to understand the reason for reduced yield and recovery at longer milling times; use of other solvents or other extraction techniques is necessary.

## CHAPTER 4

### NITRATION OF OTHER AROMATIC COMPOUNDS

The application of the mechanochemical method to nitration of other aromatic compounds has been explored by using three other substrates: naphthalene, anisole, and aniline.

#### 4.1 Naphthalene Nitration

##### 4.1.1 Experimental

Naphthalene was nitrated in a series of experiments using aluminum chloride and molybdenum oxide as catalysts. Aluminum chloride catalyzed nitration was carried out in Spex 6850 freezer mill using a single steel rod magnetically oscillated inside a steel milling vial immersed in liquid nitrogen. The MoO<sub>3</sub> catalyzed experiments were performed in the air-cooled shaker mill and in Union Process 01HD attritor mill at room temperature and cryogenically. Steel balls of 3/8 inch diameter were used as milling media in both mills. The milling conditions for this series of experiments are summarized in Table 4.1. The materials used were naphthalene (Alpha Aesar, 99 % pure, solid at room temperature), sodium nitrate (Alfa Aesar, 99%), aluminum chloride (Sigma-Aldrich, 99.99 pure), and molybdenum oxide (Alfa-Aesar, 99.95 % pure). For subsequent analysis, organic products were extracted with ethyl acetate (Alfa Aesar, 99.5 % pure).

**Table 4.1** Milling Equipment and Operating Conditions

| Milling parameters                               | Spex 8000D  | Spex 6850 Freezer Mill   | Union Process 01HD  |
|--|---|--|---|
| Sample mass                                      | 1.5 – 3 g   | 1.5 g  | 50 g  |
| Milling media                                    | 3/8 in carbon steel balls   | single 3/8 x 2 in impactor   | 3/8 in carbon steel balls                                 |
| Milling vial                                     | 60 mL   | 7/8 in x 3 7/8 in  | 1.4 L   |
| Ball-to-powder mass ratio (BPR, C <sub>R</sub> ) | 10 – 50   | N/A  | 36  |
| Milling times                                    | up to 3 hours, continuous   | 15 cycles of 10 min intervals milling at 15 Hz. Total active milling time, max. 2.5 h. | Up to 3 hours, continuous                                 |
| Milling atmosphere                               | Vials loaded under argon  | Vials not hermetically sealed; effectively milled under nitrogen                       | Nitrogen gas flow   |
| Cooling  | Jets of room temperature compressed air directed at the milling vials | Milling vials immersed in liquid nitrogen  | Jacket flow of room temperature water, or liquid nitrogen |

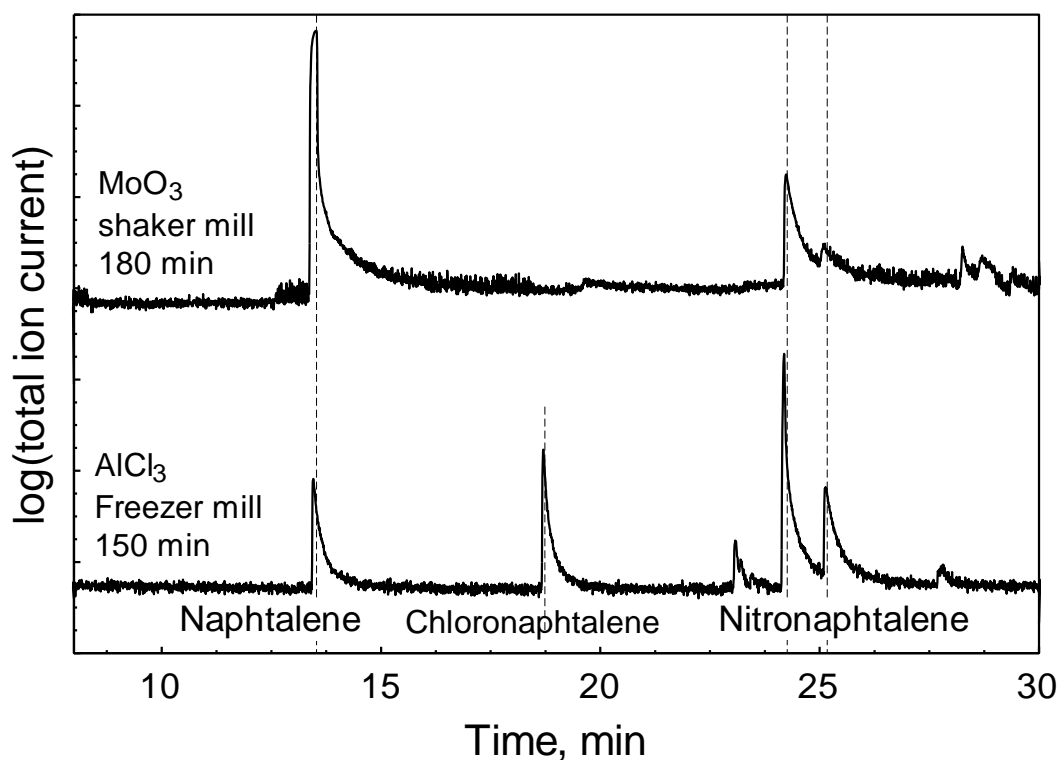
The organic products were analyzed by gas chromatography and mass spectrometry using a HP 6890 GC-MS analyzer (heating profile: 40 °C to 300 °C at 5 K/min). Product species were identified using the NIST Mass Spectral Library (NIST 08), and relative concentrations were determined using GC peak integration. Yields were estimated by evaluating the ratio of the product peak areas to the combined product and leftover substrate peak areas, according to equation 3.1. Selectivities were estimated as ratios of product peak areas to the sum of all product peak areas.

#### 4.1.2 Results and Discussion

Naphthalene was selected as a material that is relatively easy to handle and nitrate. Currently, nitration of naphthalene is achieved by exposing naphthalene to nitric and sulfuric acids; the amount of sulfuric acid may be reduced by properly selecting a solvent, e.g., dichloromethane [85]. Here, naphthalene was nitrated by ball milling with sodium nitrate. Aluminum chloride, AlCl<sub>3</sub> was selected as a well-known strong Lewis acid [86]. This experiment was performed at cryogenic

temperature, and the result is illustrated in Figure 4.1 (bottom trace). The combined yield of nitronaphthalene isomers in that experiment was 55.4% based on the recovered naphthalene and derivatives. Although a high yield of nitronaphthane was obtained, it was observed that significant amounts undesirable chlorinated products (17.2% yield) formed as well. For comparison, the reaction was also carried out in a test tube in  $\text{CCl}_4$ . The liquid phase reaction also produced nitro- and chloro- naphthalenes, but the yields were very small, less than 1% each.

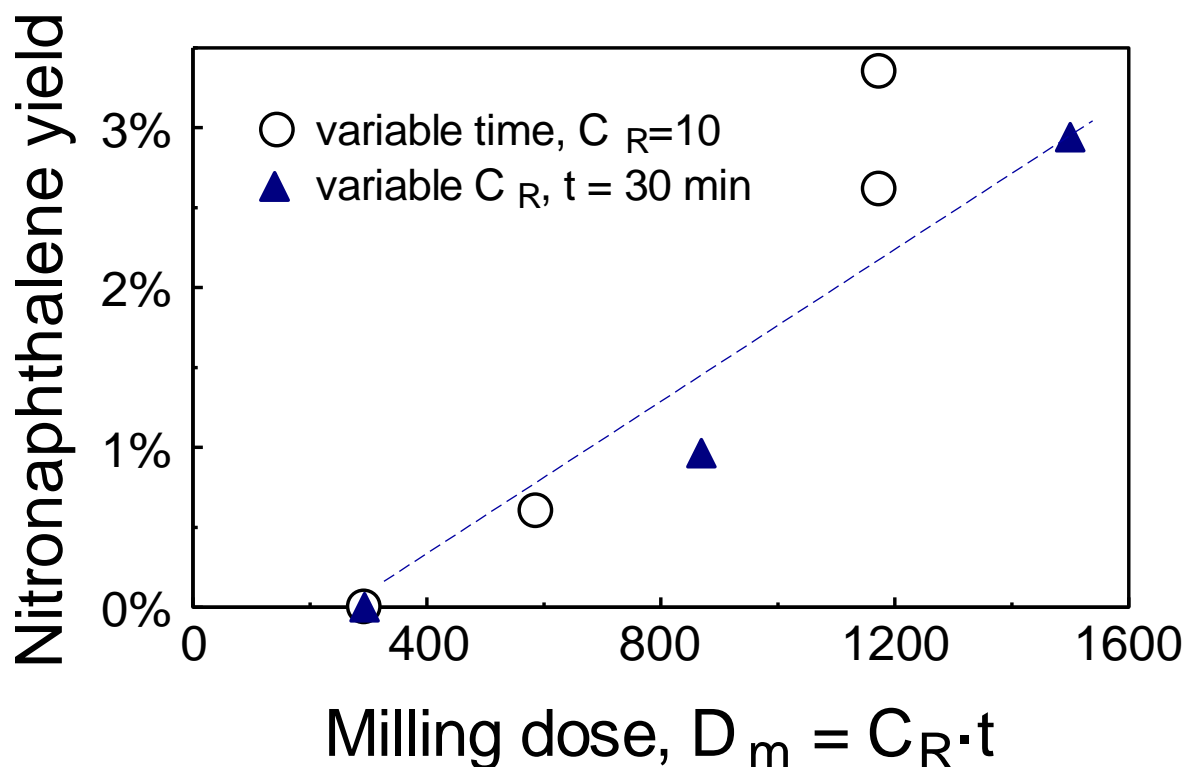
Using  $\text{MoO}_3$  as weak Lewis acid catalyst, the nitration was carried out in the shaker mill at room temperature and in attritor mill at room temperature and cryogenically. The result is shown in Figure 4.1 (top trace). Although the yield is considerably less (note the logarithmic vertical scale), major byproducts are absent.



**Figure 4.1** Sample GC traces for the products of cryogenic naphthalene nitration using  $\text{AlCl}_3$  (bottom trace) and room temperature shaker mill nitration using  $\text{MoO}_3$  (top trace).

Although other metal oxides were tested as possible much weaker, but more environmentally friendly candidate Lewis acid catalysts [87], only  $\text{MoO}_3$  showed any sign of reaction.





**Figure 4.2** Nitronaphthalene yield as a function of milling dose for experiments carried out in the shaker mill. Charge ratio,  $C_R$  is the ball to powder mass ratio.

To examine how nitronaphthalene yield with  $\text{MoO}_3$  as catalyst depends on milling conditions, milling time and the charge ratio were systematically varied a set of shaker mill experiments. Samples were milled at a constant charge ratio  $C_R=10$  for 30, 60, and 120 minutes, and for 30 minutes at charge ratios of 10, 30, and 50. The results are presented in Figure 4.2 using the concept of a milling dose introduced earlier [88-90]. Milling dose is defined as the energy transferred from the milling tools (e.g., milling balls) to the material being milled. For the simplest estimate, the charge ratio,  $C_R$ , multiplied by the milling time,  $t$ , gives a value proportional to the milling dose [88] for a given mill. Figure 4.2 shows a nearly linear increase in yield as a function of the milling dose with a maximum yield near 3 %, but no indication of a final steady state conversion reached. The two hour attritor mill run at room temperature gave 2.18% yield comparable to 2.69% yield of the two hour shaker mill run. The liquid nitrogen-cooled attritor mill run did not produce detectable amounts of nitronaphthalene. The product yields achieved in these early experiments were low. Based on the (subsequent) work on toluene nitration, it can be

assumed that the yields can be substantially increased by increasing the relative amounts of  $\text{MoO}_3$  catalyst. It is also worth mentioning that the nitronaphthalene yields were higher than nitrotoluene yields obtained under the identical conditions, as can be expected considering that naphthalene is more activated towards electrophilic aromatic substitution than toluene.

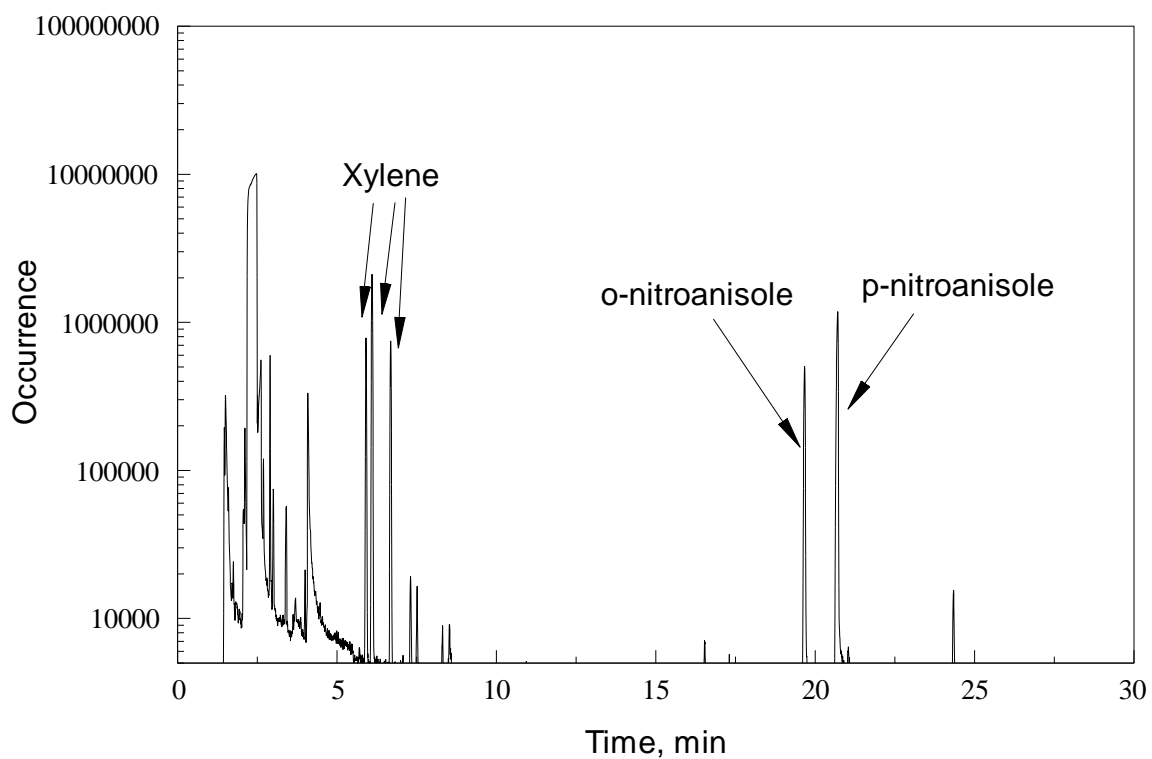
## **4.2 Other Compounds**

### **4.2.1 Experimental**

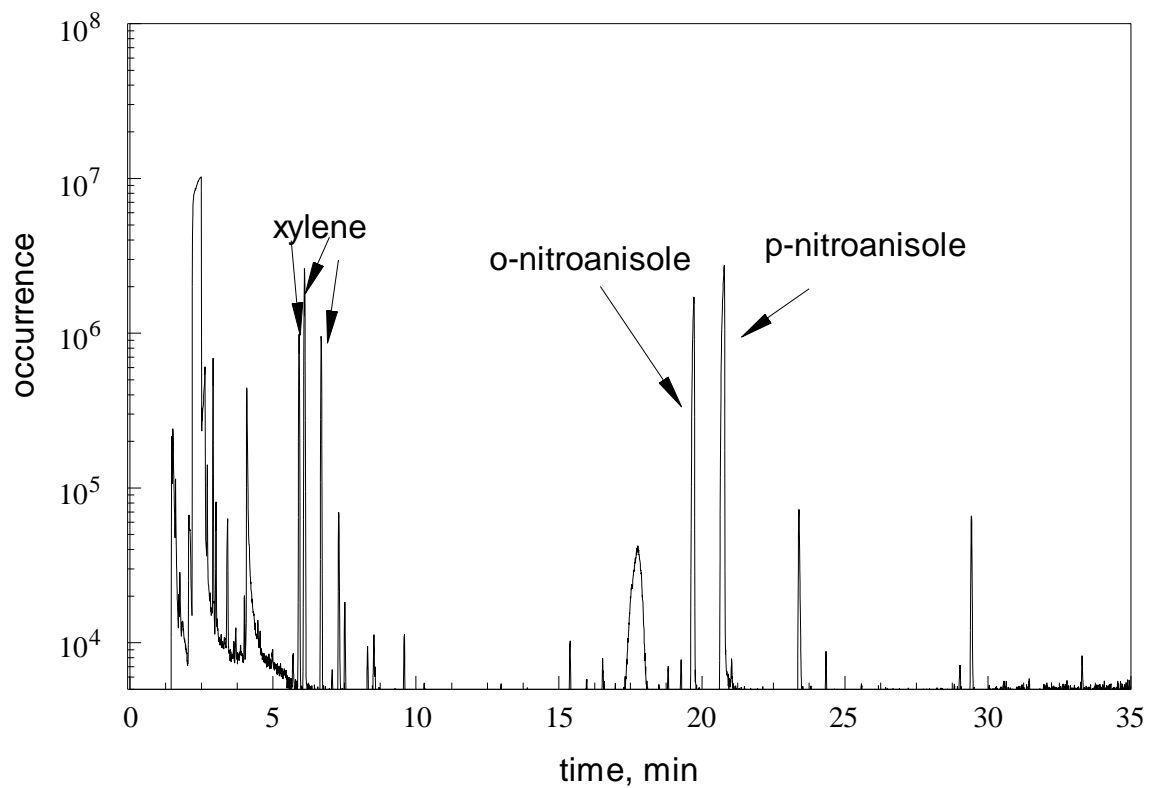
Planetary mill was employed to explore mechanochemical nitration of three other compounds: anisole, aniline, and glycerin. Two samples were prepared for each compound. In each pair of samples one contained 41.67 g of pure  $\text{MoO}_3$  catalyst with 1.67 g of  $\text{NaNO}_3$ , the other had  $\text{MoO}_3$ - $\text{SiO}_2$  catalyst with 30% silica. The total mass of the catalyst and the mass of  $\text{NaNO}_3$  was the same. 0.5 ml of liquid substrate was added to each vial. All samples were milled for 2 hours with 6 mm steel balls, using the intermediate temperature control protocol, i.e., continuous milling using cooling fins.

### **4.2.2 Results**

Mechanochemical nitration of anisole produced a mixture of two isomers of nitroanisole: ortho- and para-. No meta- isomer was detected, reflecting the strongly ortho- para-directing nature of anisole. The total yields were 9.3% and 35.1% for the pure  $\text{MoO}_3$  and  $\text{MoO}_3$ - $\text{SiO}_2$  catalyst samples respectively. The GC traces of the two samples are shown in Figures 4.3 and 4.4.



**Figure 4.3** GC trace for the anisole nitration sample. Catalyst: pure  $\text{MoO}_3$



**Figure 4.4** GC trace for the anisole nitration sample. Catalyst: 70%  $\text{MoO}_3$  30%  $\text{SiO}_2$

It is worth pointing out that in both cases no unreacted anisole was recovered, thus it can be argued that the relatively low yields were due to losses of anisole and/or nitroanisole, rather than incomplete conversion. The selectivity was higher in the case of pure  $\text{MoO}_3$  catalyst; no byproducts have been detected. Nitration of aniline and glycerin, on the other hand, did not produce detectable amounts of the nitro- derivatives of either compound.

### **4.3 Secondary Nitration**

Secondary nitration has been observed in a number of molybdenum oxide nitration experiments with anisole and toluene. Addition of a nitro- group strongly deactivates aromatic compounds toward electrophilic substitution, therefore the observed yields of dinitro- products have been rather low. In the case of anisole nitration dinitroanisole yield (based on the initial amount of anisole) was 0.23% for the sample with 30% silica and 0.057% for the sample with pure  $\text{MoO}_3$ . In the toluene nitration experiments dinitrotoluene was detected whenever substantial amounts of nitrotoluene were produced but its yields stayed under 1%.

## **CHAPTER 5**

### **CONCLUSIONS**

This study investigated mechanochemical nitration of aromatic compounds with a specific focus on the nitration of toluene because of the considerable industrial significance of nitrotoluene. The feasibility of this approach has been clearly demonstrated and practically significant product yields have been obtained. A number of important parameters affecting the desired product yield and selectivity have been identified and studied. These include the ratios of the reactants to each other and to the catalyst, milling time and temperature, milling media size and density. The enhancement of the MoO<sub>3</sub> catalytic activity by adding silica has been explored and the optimum fraction of silica has been identified. The mechanism of this process appears to be complex and still needs to be explored in the future studies, but this study did provide several clues which promise to be useful in that quest.

## APPENDIX

### DERIVATION OF THE MILLING DOSE FORMULA

Consider collision frequency by analogy to the collision frequency of molecules given by the molecular theory for collision of molecules in a gas. In that case, the collision frequency is:

$$Z_{ii} = \frac{\sqrt{2}}{2} \pi d^2 \langle c \rangle \left( \frac{N}{V} \right)^2$$

Where  $d$  is molecule diameter,  $N$  is the number of molecules,  $V$  is volume, and  $c$  is speed. For the present estimate, the balls can be treated as molecules, so that the  $d$  and  $N$  are respectively diameter and number of milling balls. Note that balls in the milling vial, unlike molecules in an ideal gas, move together. Thus, multiple collisions involve more than two balls at the same time. This effect is strong, but is not accounted for in the present estimate. The effect becomes stronger as the number of balls increase, while their size is reduced to maintain a constant BPR. Thus, the effect of ball size on the collision frequency is expected to be underestimated.

With this in mind, the milling dose can be expressed as

$$D = Z_{ii} \cdot \left( \frac{mv^2}{2} \right) t$$

$$D \sim d^2 N^2 \cdot \left( \frac{mv^2}{2} \right) t \sim d^2 N \cdot M \cdot t,$$

Where mass of balls  $M=N \cdot m$ , and the effect of velocity  $v$  is removed taking into account that the velocity is driven by the vial motion and thus is the same for all experiments using

the same mill. It is further assumed that differences in volume are negligible for different cases.

$$M = Nm = N \cdot \rho \frac{\pi d^3}{6}$$

$$D \sim d^2 N \cdot N \cdot \rho \frac{\pi d^3}{6} \cdot t$$

Number of balls can be taken as  $N = \frac{M}{\rho \frac{\pi d^3}{6}}$

Thus

$$D \sim d^2 \frac{M^2}{\rho \frac{\pi d^3}{6}} \cdot t = \frac{M^2}{\rho \frac{\pi d}{6}} \cdot t \sim \frac{M^2}{\rho d} \cdot t$$

Finally, for the same mass of balls,

$$D \sim \frac{t}{\rho d}$$

Considering collective ball motion and significant role of collisions involving simultaneously more than two balls, it is likely that the effect of ball size  $d$  is stronger than estimated above.

## REFERENCES

1. Topchiev, A.V., *Nitration of Hydrocarbons and Other Organic Compounds*. 2013: Elsevier Science.
2. Millar, A. W., et al., *New Synthesis Routes for Energetic Materials Using Dinitrogen Pentoxide [and Discussion]*. Philosophical Transactions: Physical Sciences and Engineering, 1992(1654): p. 305.
3. Schofield, K., *Aromatic Nitration*. 1980: Cambridge University Press.
4. Agrawal, J.P. and Hodgson, R. D. *Organic Chemistry of Explosives*. Organic Chemistry of Explosives. 2007. 1-384.
5. Ono, N., *The Nitro Group in Organic Synthesis*. 2003, New York: Wiley.
6. Albadi, J. F.S., Bahareh Ghabezi, Tayebbeh Seiadatnasab, *Melamine trisulfonic acid catalyzed regioselective nitration of aromatic compounds with sodium nitrate under solvent-free conditions*. Arabian Journal of Chemistry, 2012. **10**: p. S509-S513.
7. Ledgard, J., *The Preparatory Manual of Explosives Fourth Edition*. 2014: Jared B. Ledgard.
8. Akhavan, J., *The Chemistry of Explosives*. 2015: Royal Society of Chemistry.
9. *Nitrobenzene and Nitrotoluene*, in *Encyclopedia of chemical processing and design*, J.J. McKetta, Editor., M. Dekker.
10. Zukas, J.A. and Walters, W. *Explosive Effects and Applications*. 2013: Springer New York.
11. Williams, D.F. and Schmitt, W. H. *Chemistry and Technology of the Cosmetics and Toiletries Industry*. 1996: Springer.
12. *Nitrobenzene and nitrotoluene*, in *Kirk-Othmer encyclopedia of chemical technology*, J.I. Kroschwitz, Editor. 2004, Wiley-Interscience: Hoboken, N.J.
13. Carey, F. A., *Organic Chemistry*. 2nd ed. 1992: McGraw-Hill, Inc.
14. Vassena D., K.A., Prins R., *Potential routes for the nitration of toluene and nitrotoluene with solid acids*. Catalysis Today, 2000. **60**: p. 275-287.
15. Meyers, R.A., in *Encyclopedia of Environmental Analysis and Remediation*. 1998, Wiley: New York.
16. Ganjala, V.S.P., et al., *Eco-friendly nitration of benzenes over zeolite- $\beta$ -SBA-15 composite catalyst*. Catalysis Communications, 2014. **49**: p. 82-86.
17. Peng, X., Suzuki, H., and Lu, C., *Zeolite-assisted nitration of neat toluene and chlorobenzene with a nitrogen dioxide/molecular oxygen system. Remarkable enhancement of para-selectivity*. Tetrahedron Letters, 2001. **42**(26): p. 4357-4359.
18. Adamiak, J.T., Skupinski, W., *Interaction of nitromethane with MoO<sub>3</sub>/SiO<sub>2</sub> and its influence on toluene nitration*. Catalysis Communications, 2012. **29**: p. 92-95.
19. Kogelbauer, A., Prins, D.V., R., Armor, J. N., *Solid acids as substitutes for sulfuric acid in the liquid phase nitration of toluene to nitrotoluene and dinitrotoluene*. Catalysis Today, 2000. **55**: p. 151-160.
20. Gong, S., et al., *Stable and eco-friendly solid acids as alternative to sulfuric acid in the liquid phase nitration of toluene*. Process Safety and Environmental Protection, 2014. **92**(6): p. 577-582.
21. Adamiak, J., et al., *Characterization of a novel solid catalyst, H<sub>3</sub>PO<sub>4</sub>/MoO<sub>3</sub>/SiO<sub>2</sub>, and its application in toluene nitration*. Journal of Molecular Catalysis A: Chemical, 2011. **351**: p. 62-69.
22. Peng, X. H. S., Lu, C., *Zeolite-assisted nitration of neat toluene and chlorobenzene with a nitrogen dioxide/molecular oxygen system. Remarkable enhancement of para-selectivity*. Tetrahedron Letters, 2001. **42**: p. 4357-4359.



23. Pervez, H., et al., *Selective functionalisation. Part 10. The nitration of phenols by pyridine derivatives carrying a transferable nitro group* 1 Part 9. S.O. Onyiriuka and C.J. Suckling, *J. Org. Chem.*, 1986, 51, 1900. *Tetrahedron*, 1988. **44**(14): p. 4555-4568.
24. Takacs, L., *The historical development of mechanochemistry*. *Chemical Society Reviews*, 2013. **42**(18): p. 7649-7659.
25. James, S.L., Bolm, C., Braga, D., Collier, P., Friiç, T., Grepioni, F., Harris, K.D.M., Hyett, G., Jones, W., Krebs, A., MacK, J., Maini, L., Orpen, A.G., Parkin, I.P., Shearouse, W.C., Steed, J.W., Waddell, D.C. *Mechanochemistry: Opportunities for new and cleaner synthesis*. *Chemical Society Reviews*, 2012. **41**: p. 413-447.
26. Boldyrev, V.V. and Tkáčová, K., *Mechanochemistry of solids: Past, present, and prospects*. *Journal of Materials Synthesis and Processing*, 2000. **8**(3-4): p. 121-132.
27. Frišćić, T., *New opportunities for materials synthesis using mechanochemistry*. *Journal of Materials Chemistry*, 2010. **20**(36): p. 7599-7605.
28. Frišćić, T., *Supramolecular concepts and new techniques in mechanochemistry: Cocrystals, cages, rotaxanes, open metal-organic frameworks*. *Chemical Society Reviews*, 2012. **41**(9): p. 3493-3510.
29. Kaupp, G., *Mechanochemistry: The varied applications of mechanical bond-breaking*. *CrystEngComm*, 2009. **11**(3): p. 388-403.
30. Baláž, P., *Mechanochemistry in nanoscience and minerals engineering*. *Mechanochemistry in Nanoscience and Minerals Engineering*. 2008. 1-413.
31. Baláž, P., et al., *Hallmarks of mechanochemistry: From nanoparticles to technology*. *Chemical Society Reviews*, 2013. **42**(18): p. 7571-7637.
32. Huot, J., et al., *Mechanochemical synthesis of hydrogen storage materials*. *Progress in Materials Science*, 2013. **58**(1): p. 30-75.
33. Baláž, P., et al., *Chalcogenide mechanochemistry in materials science: insight into synthesis and applications (a review)*. *Journal of Materials Science*, 2017. **52**(20): p. 11851-11890.
34. Baláž, P., et al., *Mechanochemical Solvent-Free Synthesis of Quaternary Semiconductor Cu-Fe-Sn-S Nanocrystals*. *Nanoscale Research Letters*, 2017. **12**(1).
35. Côa, F., et al., *Coating carbon nanotubes with humic acid using an eco-friendly mechanochemical method: Application for Cu(II) ions removal from water and aquatic ecotoxicity*. *Science of the Total Environment*, 2017. **607-608**: p. 1479-1486.
36. Dong, B.X., et al., *Mechanochemical synthesis of CO<sub>x</sub>-free hydrogen and methane fuel mixtures at room temperature from light metal hydrides and carbon dioxide*. *Applied Energy*, 2017. **204**: p. 741-748.
37. Lomovsky, O.I., Lomovskiy, I.O., and Orlov, D.V. *Mechanochemical solid acid/base reactions for obtaining biologically active preparations and extracting plant materials*. *Green Chemistry Letters and Reviews*, 2017. **10**(4): p. 171-185.
38. Siddhanti, D.A., et al., *The safer and scalable mechanochemical synthesis of edge-chlorinated and fluorinated few-layer graphenes*. *Journal of Materials Science*, 2017. **52**(20): p. 11977-11987.
39. Takacs, L., *The mechanochemical reduction of AgCl with metals*. *Journal of Thermal Analysis & Calorimetry*, 2007. **90**(1): p. 81-84.
40. Karolus, M., E. Jartych, and D. Oleszak, *Structure and magnetic properties of nanocrystalline Fe-Mo alloys prepared by mechanosynthesis*. *Acta Physica Polonica A*, 2002. **102**(2): p. 253-258.
41. Dreizin, E.L. and Schoenitz, M., *Mechanochemically prepared reactive and energetic materials: a review*. *Journal of Materials Science*, 2017. **52**(20): p. 11789-11809.
42. Dario, B., et al., *Making crystals with a purpose; a journey in crystal engineering at the University of Bologna*. *IUCrJ*, Vol 4, Iss 4, Pp 369-379 (2017), 2017(4): p. 369.
43. Kaupp, G., Naimi-Jamal, M.R., and Schmeyers, J., *Solvent-free Knoevenagel condensations and Michael additions in the solid state and in the melt with quantitative yield*. *Tetrahedron*, 2003. **59**(21): p. 3753-3760.

44. Declerck, V., et al., *Solvent-free synthesis of peptides*. Angewandte Chemie - International Edition, 2009. **48**(49): p. 9318-9321.
45. Cheng, X., et al., *Solvent-free synthesis of dihydrofuran-fused [60]fullerene derivatives by high-speed vibration milling*. Chinese Chemical Letters, 2005. **16**(10): p. 1327-1329.
46. İçli, B., et al., *Synthesis of molecular nanostructures by multicomponent condensation reactions in a ball mill*. Journal of the American Chemical Society, 2009. **131**(9): p. 3154-3155.
47. Braga, D., et al., *Mechanochemical preparation of molecular and supramolecular organometallic materials and coordination networks*. Dalton Transactions, 2006. **6**(10): p. 1249-1263.
48. Štrukil, V., et al., *Towards an environmentally-friendly laboratory: dimensionality and reactivity in the mechanosynthesis of metal-organic compounds* Electronic supplementary information (ESI) available: PXRD patterns, FTIR spectra and solid-state NMR spectra for selected materials. CCDC 792744 and CCDC 792745. For ESI and crystallographic data in CIF or other electronic format see DOI: 10.1039/c0cc03822a. Chemical Communications, 2010. **46**(48): p. 9191-9193.
49. Todres, Z.V., *Organic Mechanochemistry and Its Practical Applications*. Boca Raton, FL: CRC Press Taylor and Frances Group.
50. Balaz, P., *Mechanochemistry in Nanoscience and Minerals Engineering*. 2008, Berlin: Springer-Verlag.
51. Choksi, T. and Greeley, J., *Partial Oxidation of Methanol on MoO<sub>3</sub> (010): A DFT and Microkinetic Study*. ACS Catalysis, 2016. **6**(11): p. 7260-7277.
52. Tatibouet, J.M., *A Structure-Sensitive Oxidation Reaction: Methanol on Molybdenum Trioxide Catalysis*. Journal of Catalysis, 1981. **72**(2): p. 375-378.
53. Smith, R.L. and Rohrer, G.S., *An atomic force microscopy study of the morphological evolution of the MoO<sub>3</sub> (010) surface during reduction reactions*. Journal of Catalysis, 1996. **163**(1): p. 12-17.
54. Albright, L.F., *Nitration*, in *Kirk-Othmer Encyclopedia of Chemical Technology*. 2000, John Wiley & Sons, Inc.
55. Hoggett, J.G., Penton, J.R., Schoefield, K., *Nitration and aromatic reactivity*. 1971, Cambridge University Press: Cambridge.
56. Esteves, P. M., Cardoso, S.P., Barbosa, A.G.H., Laali, K.K., Rasul, G., Pra-kash, G.K.S., Olah, G.A., *Unified mechanistic concept of electrophilic aro-matic nitration: Convergence of computational re-sults and experimental data*. Journal of the American Chemical Society, 2003. **125**: p. 4836-4849.
57. Booth, G., *Nitro Compounds, Aromatic*, in *Ullmann's Encyclopedia of Industrial Chemistry*. 2000, Wiley-VCH Verlag GmbH & Co. KGaA.
58. Lu, K.T., Lin, P.C., Hwang, K.L., *Critical runaway conditions and stability criterion of RDX manufacture in continuous stirred tank re-actor*. Journal of Loss Prevention in the Process Industries, 2005. **18**: p. 1-11.
59. Zhang, M., Song, K., Wang, Z., Zhao, Q., Li, S., Ye, Z., *Biological treatment of 2,4,6-trinitrotoluene (TNT) red water by immobilized anaerobic-aerobic microbial filters*. Chemical Engineering Journal, 2015. **259**: p. 876-884.
60. Ludwigk, R., Kist, C.P., Lopes, A.C., Cavasotto, T., Silva, D.C., Barreto-Rodrigues, M., *Characterization and photocatalytic treatability of red water from Brazilian TNT industry*. Journal of Hazardous Materials, 2015. **293**: p. 81-86.
61. Tu, S., Hu, P., Meng, Z., Ran, H., Zhang, Y., *Preparation of amine-modified silica foams and their adsorption behaviors toward TNT red water*, *Colloids and Surfaces. Physicochemical and Engineering Aspects*, 2015. **481**: p. 493-499.

62. Pouretedal, H.R., Alikhasti, M, Mahmoodi, H., *Treatment of TNT red water by chemical-modified carbon adsorbent prepared from cheap raw materials of pine tree wood*. Desalination and Water Treatment: p. 1-10.
63. Millar, R. W., Arber, A. W., Claridge, R.P., Endsor, R.M., Hamid, J., *Clean nitrations using dinitrogen pentoxide (N<sub>2</sub>O<sub>5</sub>)-A UK perspective*. Energetic Materials: Chemistry, Hazards and Environmental Aspects, 2011: p. 77-106.
64. Millar, R. W., et al., *Clean nitrations: Novel syntheses of nitramines and nitrate esters by nitrodesilylation reactions using dinitrogen pentoxide (N<sub>2</sub>O<sub>5</sub>)*. Tetrahedron, 1997. **53**: p. 4371-4386.
65. Holt, P., Sanderson, A.J., Wesson, P., Worthington, J. *Development of an Efficient and Green TNT Manufacturing Process, 2004 Insensitive Munitions and Energetic Materials*. 2004, Materials Technical Symposium: San Francisco, CA.
66. Garay, A. L., James, S.L., *Solvent-free synthesis of metal complexes*. Chemical Society Reviews,, 2007. **36**: p. 846-855.
67. Kaupp, G., *Mechanochemistry: The varied applications of mechanical bond-breaking*. CrystEngComm, 2009. **11**: p. 388-403.
68. Friić, T., *New opportunities for materials synthesis using mechanochemistry*. Journal of Materials Chemistry, 2010. **20**: p. 7599-7605.
69. Wang, G.W., *Mechanochemical organic synthesis*. Chemical Society Reviews,, 2013. **42**: p. 7668-7700.
70. Ji, L., C.Q., Liu, M., Chen, X. *Highly Efficient Nitration of phenolic compounds using some nitrates and oxalic acid under solvent free conditions*. Journal of Chemical Research, 2011. **35**(2): p. 101-103.
71. Skupiński, W. and Malesa, M. *An infrared study on the MoO<sub>3</sub>/SiO<sub>2</sub> catalytic system employed in toluene nitration*. Applied Catalysis A: General, 2002. **236**(1-2): p. 223-234.
72. Kemdeo, S.M., Sapkal, V.S. and Chaudhari, G.N. *TiO<sub>2</sub>-SiO<sub>2</sub> mixed oxide supported MoO<sub>3</sub> catalyst: Physicochemical characterization and activities in nitration of phenol*. Journal of Molecular Catalysis A: Chemical, 2010. **323**(1-2): p. 70-77.
73. Kemdeo, S.M., *MoO<sub>3</sub>/SiO<sub>2</sub>-ZrO<sub>2</sub> catalyst: Effect of calcination temperature on physico-chemical properties and activities in nitration of toluene*. Bulletin of Chemical Reaction Engineering and Catalysis, 2012. **7**(2): p. 92-104.
74. Adamiak, J., Tomaszewski, W. and Skupiński, W. *Interaction of nitromethane with MoO<sub>3</sub>/SiO<sub>2</sub> and its influence on toluene nitration*. Catalysis Communications, 2012. **29**: p. 92-95.
75. Ward, T.S., W.C., Schoenitz, M., Dave, R.N., Dreizin, E.L. *A study of mechanical alloying processes using re-active milling and discrete element modeling*. Acta Materialia, 2005. **53**: p. 2909-2918.
76. Jiang, X., M.A.T., Schoenitz, M., Dave, R.N., Dreizin, E.L., *Mechanical alloying and reactive milling in a high energy planetary mill*. Journal of Alloys and Compounds, 2009. **478**: p. 246-251.
77. Santhanam, P.R., Dreizin, E. L., *Predicting conditions for scaled-up manufacturing of materials prepared by ball milling*. Powder Technology, 2012. **201**: p. 401-411.
78. Agrawal, J.P. and Hodgson, R.D. *Organic Chemistry of Explosives*. 2007, Chichester, UK: John Wiley and Sons. 1-384.
79. Albadi, J., et al., *Melamine trisulfonic acid catalyzed regioselective nitration of aromatic compounds with sodium nitrate under solvent-free conditions*. Arabian Journal of Chemistry, 2012. **10**: p. S509-S513.
80. Dugal, M., *Nitrobenzene and nitrotoluene*, in *Kirk-Othmer encyclopedia of chemical technology*, J.I. Kroschwitz, Editor. 2004, Wiley-Interscience: Hoboken, N.J.
81. Vassena, D., Kogelbauer, A., and Prins, R. *Potential routes for the nitration of toluene and nitrotoluene with solid acids*. Catalysis Today, 2000. **60**: p. 275-287.

82. Lagoviyer, O.S., Krishtopa, L., Schoenitz, M., Trivedi, N. J., Dreizin, E. L.,  
*Mechanochemical Nitration of Aromatic Compounds*. Journal of Energetic Materials,  
2017: p. 1-11.
83. Umbrajkar, S.M., et al., *Effect of temperature on synthesis and properties of aluminum-  
magnesium mechanical alloys*. Journal of Alloys and Compounds, 2005. **402**(1-2): p. 70-  
77.
84. Rajagopal, S., Marzari, J.A., and Miranda, R. *Silica-alumina-supported mo oxide catalysts:  
Genesis and demise of brønsted-lewis acidity*. Journal of Catalysis, 1995. **151**(1): p. 192-  
203.
85. Kameo, T. and Hirashima, T. *Mononitration of naphthalene with nitric acid in inert solvents*.  
Chem. Express, 1986. **1**(6): p. 371-4.
86. Kobayashi, S., Busujima, T. and Nagayama, S. *A novel classification of Lewis acids on the  
basis of activity and selectivity*. Chemistry - A European Journal, 2000. **6**(19): p. 3491-  
3494.
87. Corma, A. and García, H. *Lewis acids as catalysts in oxidation reactions: From homogeneous  
to heterogeneous systems*. Chemical Reviews, 2002. **102**(10): p. 3837-3892.
88. Ward, T.S., et al., *A study of mechanical alloying processes using reactive milling and  
discrete element modeling*. Acta Materialia, 2005. **53**(10): p. 2909-2918.
89. Jiang, X., et al., *Mechanical alloying and reactive milling in a high energy planetary mill*.  
Journal of Alloys and Compounds, 2009. **478**(1-2): p. 246-251.
90. Santhanam, P.R. and Dreizin, E.L. *Predicting conditions for scaled-up manufacturing of  
materials prepared by ball milling*. Powder Technology, 2012. **201**: p. 401-411.